# Evolutionary Models

Models of the ocean biology generally attempt to mimic the structure of the ocean as we understand it from a very sparse data base. For example, suppose we have constructed an NPPZ model, apply a seasonal cycle, and find one species appearing in spring and the other in fall (figure 6.1a). But it is quite possible that another species with characteristics intermediate bewteen the two could end up outcompeting, resulting in a single type present for the whole year (figure 6.1b). The two species model, then, may provide a description of the phytoplankton assemblage, but cannot explain it. Rather, we have to find what physiological constraints and tradeoffs (as well as the circulation and mixing) determine spatial and temporal biogeography.

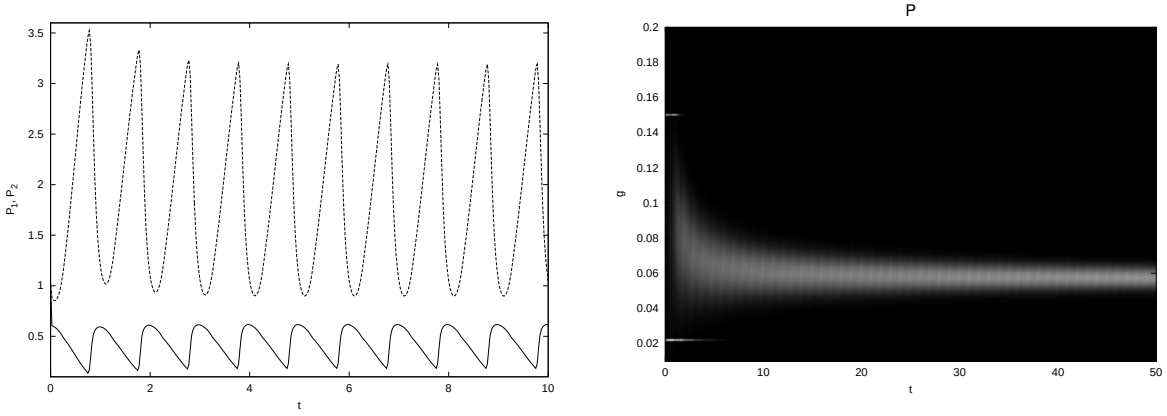


Figure 6.1: a) Time series with just two types with seasonal mixed-layer depth variations b) Time series with the two types perturbed by others with different uptake rates and grazing vulnerability. $P^{1/4}$ is plotted to enhance the contrast.

This example indicates the importance of going beyond models with fixed traits and beginning to consider models which populate a wide range of trait space or which allow mutable traits. The former were discussed briefly in previous chapters, but will be expanded upon here. However, the context is different; rather than trying to see how a complex system with many species could be represented, we are now exploring how evolution/ natural selection, in conjunction with advection and mixing, will structure oceanic ecosystems.

"Natural selection" occurs when phenotype (observable charateristics) variations lead to individuals which are more likely to reproduce and survive than others with less favorable characteristics. These traits must be inheritable, but with the possibility of alteration by mutation. Thus a model which includes evolutionary processes would have:

- a set of variables $\mathbf{s} = \{s_1, s_2, \ldots\}$ which specify the phenotype of the organism. in the model, these "trait variables" will set all of the vital rates (e.g., growth rates, half-saturation constants, vulnerability to predation, etc.). The biomass density can be treated as a function over space, time, and this "trait-space"

$$b(\mathbf{x}, t|s_1, s_2, ...)$$

- rates of survival and reproduction which depend on the environmental conditions and vary with phenotype

$$\mathcal{R} = \mathcal{R}(\mathbf{s}|E) \quad , \quad \mathcal{R}(\mathbf{s}_1|E) \neq \mathcal{R}(\mathbf{s}_2|E)$$

- inheritance of traits, implying new organisms have the same values of $\mathbf{s}$ as the parents

$$\frac{\partial}{\partial t} b(\mathbf{s}) = \mathcal{R}(\mathbf{s}|E) b(\mathbf{s}) \ldots$$

- and the potential for mutation. For a continuous trait space, we could think of this as a random walk or diffusive process, though that is undoubtably a great oversimplification. If we associate mutation with reproductive events (occuring at a rate proportions to $g$), then we could write

$$\frac{\partial}{\partial t} b(s) = \int ds' g(s') M(s|s') b(s') \ldots$$

with the expectation that the probability distribution $M$ is very narrow; expanding then gives an alternative form

$$\frac{\partial}{\partial t} b(s) = g(s) b(s) + \frac{\partial^2}{\partial s^2} m g b \ldots$$

with $m$ being half the standard deviation of $M$. The differential form has the disadvantage, common to diffusion problems, of having a finite albeit tiny probability of transforming a trait into any possible value. Discretizations slow the process; however, if that's a concern, the integral form can be used to bound the changes. We could also consider a nonlinear form expressing the likelihood of offspring of type $s$ arising from parents with types $s'$ and $s''$. But we should also expect that, even without nutation, offspring will have some spread in characteristics around that of the parents, so that $m$ above includes both natural variability in traits and changes induced by mutation. For simplicity, we use a standard diffusion in trait space, with the expectation that it will give a sense of the effects of mutation and trait variability.

MATH NOTE

The approximation of

$$F(s) = \int ds' M(s|s') f(s')$$

when $M(s|s')$ is strongly peaked around $s = s'$ but with properties depending on $s$ and/or $s'$ is closely related to the Fokker-Planck problem in chapter xx. We split the kernel

$$M(s|s') = \frac{A(s,s')}{\sigma(s,s')} D(\frac{s'-s}{\sigma(s,s')})$$

where $D/\sigma$ is a peaked function with order one moments and $\sigma(s,s')$ is small. $s$ is a parameter, so we can leave it implicit and look at

$$F = \int ds' \frac{A(s')f(s')}{\sigma(s')} D(\frac{s'-s}{\sigma(s')})$$

with $\tilde{f} = A(s')f(s')$. Changing variables to $x = (s'-s)/\sigma(s')$ with $dx = ds(1 - x\sigma'(s'))/\sigma(s')$ gives

$$F = \int dx D(x) \frac{1}{1-x\sigma'} A(s+x\sigma) f(s+x\sigma)$$

recalling throughout that $\sigma = \sigma(s') \simeq \sigma(s) + x\sigma'(s)\sigma(s) + \ldots$. Now we expand for small $\sigma$ keeping to quadratic order.

$$F \simeq \int dx D(x) \left[ Af + \frac{\partial Af}{\partial s}\sigma x + \frac{1}{2}\frac{\partial^2 Af}{\partial s^2}\sigma^2 x^2 + \frac{\partial Af}{\partial s}\sigma'\sigma x^2 \right] \left[1 + x\sigma' + x^2\sigma\sigma'' + x^2\sigma'^2\right]$$

In terms of the moments of $D$ ($D_n = \int dx\, x^n D(x)$), this becomes

$$\begin{aligned} F &= D_0 A(s)f(s) + D_1 \frac{\partial}{\partial s} Af\sigma + D_2[Af\sigma\sigma'' + Af\sigma'^2 + (Af)'\sigma\sigma' + \frac{1}{2}(Af)''\sigma^2 + (Af)'\sigma\sigma'] \\ &= D_0 A(s)f(s) + D_1 \frac{\partial}{\partial s} Af\sigma + D_2 \frac{1}{2}\frac{\partial^2}{\partial s^2} Af\sigma^2 \end{aligned}$$

Putting back the first argument gives

$$F = A(s,s)f(s,s)M_0 + \frac{\partial}{\partial s'} A(s,s')f(s,s')M_1(s,s')\Big|_{s'=s} + \frac{1}{2}\frac{\partial^2}{\partial s'^2} AfM_2\Big|_{s'=s}$$

with the moments defined as

$$M_n(s,s') = \int dx' x'^n \frac{1}{\sigma(s,s')} D(\frac{x'}{\sigma(s,s')})$$

($s$ and $s'$ being constant for the integral).

Another way to think about this is that we are representing

$$M(s,s') \simeq M_0(s,s')\delta(s'-s) - M_1(s,s')\delta'(s'-s) + M_2(s,s')\delta''(s'-s)$$

## 6.1 — Dynamics in trait space

We can extend the quadraic (Lotka-Volterra) model to discuss the movement of biomass in a trait space $\mathbf{s}$:

$$\frac{\partial}{\partial t}b(\mathbf{s},t) = \left[L(\mathbf{s},E) + \int d\mathbf{s}'\big[a(\mathbf{s})G(\mathbf{s},\mathbf{s}') - G(\mathbf{s}',\mathbf{s})\big]b(\mathbf{s}')\right] b(\mathbf{s},t)$$

where the linear term $L$ includes uptake of abiotic resources ($E$) and death rates while the nonlinear terms represent the rate at which organism $\mathbf{s}$ grazes upon $\mathbf{s}'$, $G(\mathbf{s},\mathbf{s}')$, and the rate $a(\mathbf{s})$ at which grazed material is assimilated.

We can include food limitation by using the Monod form, both for uptake and grazing, replacing the latter by a functional of $b$ with a kernel

$$G(\mathbf{s},\mathbf{s}',b) = \frac{g_m(\mathbf{s})\Phi(\mathbf{s},\mathbf{s}')}{F_h(\mathbf{s}) + \int d\mathbf{s}''\Phi(\mathbf{s},\mathbf{s}'')b(\mathbf{s}'')}$$

which is itself a functional of $b$. As a mathematical note, we reiterate that the vital rates must give numbers for the possible values of the arguments; thus any nonlinearity must involve functionals of $b(\mathbf{s})$ which map a function $b(\mathbf{s})$ to a real number. Integrals like those above do precisely that: if we plug a function $b(s')$ into $\int G(s',s)b(s')ds'$ we get some real number (with units $1/T$) given a value of $s$. We are then able to use this as part of the rate calculation for $\frac{\partial}{\partial t}\ln b(s,t)$.

To represent these kinds of forms, we include the function $b$ as an argument in the various terms (including in $L$ where it can represent intra-species competition for resources)

$$\frac{\partial}{\partial t}b(\mathbf{s},t) = \left[L(\mathbf{s},E,b) + \int d\mathbf{s}'\big[a(\mathbf{s})G(\mathbf{s},\mathbf{s}',b) - G(\mathbf{s}',\mathbf{s},b)\big]b(\mathbf{s}',t)\right] b(\mathbf{s},t) \tag{6.1}$$

Note that $L(\mathbf{s},E,b)$ is a function of $\mathbf{s}$ and $E$ but a functional of $b$, as in the Monod example. In 6.1, autotrophs have traits $\mathbf{s}$ such that $L(\mathbf{s},E)$ can be positive and $G(\mathbf{s},\mathbf{s}')$ is zero for all $\mathbf{s}'$, while heterotrophs have strictly negative $L$ and regions of prey traits $\mathbf{s}'$ with positive grazing kernels $G$. Mixotrophs have the potential for both $L$ and $G$ to be positive given the right mixes of biotic and abiotic food sources.

We can include the forms above under the notation $\mathcal{R}(\mathbf{s},E,b)$ and incorporate advection and physical diffusion to arrive at

$$\frac{D}{Dt}b - \nabla\kappa\nabla b = b\mathcal{R}(\mathbf{s},E,b) + \int gMb \tag{6.2}$$

(with $E$ also potentially a functional of $b$) to determine the "evolutionarily stable strategies" (i.e., what $s$ values are selected for), how this is related to stability theory, and the effects of mutation, diffusion, and advection.

At this point, it is worth re-examining continuum vs. discrete representations. Our function $b$ measures density in trait space; if we discretize that space, we expect the biomass in some interval

$$\int_{s_0}^{s_1} b(s)ds$$

should become independent of the discretization. In the simplest form, an integral such as the grazing function

$$\int ds' G(s', s_i) b(s') \longrightarrow \sum_j G(s'_j, s_i) b(s'_j) ds'$$

a matrix multiplication with the $ds'$ ensuring the convergence.

The basic variables in the common discrete models, $\hat{b}_i$, represent in some sense $b\,ds$ so that adding new types will result in a decrease in the $\hat{b}_i$ values. In this chapter, we will deal with singular solutions (in the absence of mutation) which look like

$$b(s) = \hat{b}_i \delta(s - s_i)$$

Integrals again becomes sums

$$\int ds' G(s', s_i) b(s') \longrightarrow \sum_j G(s'_j, s_i) \hat{b}(s'_j)$$

but no longer have the $ds$ factor. The amplitudes will be sensitve to the number of types and their separation in $s$ space.

Numerically, if the solution tends towards a singular one, the values of $b$ will become very large, since $b(s_i)\, ds \simeq \hat{b}_i$ with the right-hand side having a well-defined, finite value. In addition, if $s_i$ does not fall on a discretization point, we may have non-zero values on one or both of the neighboring points with their sum times $ds$ giving the equivalent amplitude of the delta function. Thus we need to compare $\hat{b}$ to the local integral (sum times $ds$) of $b$.

These remarks caution against thinking of a point in trait space (or a discrete $\hat{b}_i$) as representing a "species." Instead. it occupies a small, but finite, volume in the space implying that the biomass would not depend on the resolution and exact placement of points if it is fine enough. By dealing with variability in the traits or phenotype – variability which affects survival and reproductive success – we are not able to assess gnetic variability and actual species diversity.

Mutation and reproductive variability will also lead to spreading of the delta function, suggesting the continuum representation will be more appropriate in that case. Indeed, the mutation integral is fine in the discretized sense

$$\frac{\partial}{\partial t} b(s_i) = R(s_i) b(s_i) + \int ds' M(s_i, s') g(s') b(s') \longrightarrow \frac{\partial}{\partial t} b_i = R_i b_i + \sum_j M(s_i, s_j) g(s_j) b_j ds$$

but fails with the singular or discrete solutions

$$\begin{aligned} \frac{\partial}{\partial t} \hat{b}_i \delta(s - s_i) &= R(s) \hat{b}_i \delta(s - s_i) + \int ds' M(s_i, s') g(s') \hat{b}_j \delta(s' - s_j) \\ &= R_i \hat{b}_i \delta(s - s_i) + \sum_j M(s_i, s_j) g(s_j) b_j ds \end{aligned}$$

The singularity on the l.h.s. can be cancelled with that on the growth rate, but the mutation term does not generally match. The discrete form will pose problems as more types are added; nevertheless, we find that for small mutation rates, the solutions often have rather narrow sharp peaks so that delta functions still provide a useful approximation to the other parts of the dynamics. We can solve with $M = 0$ and then assess the shape of the peaks *a posteriori* and determine the rates of leakage into regions which might not have been populated with the initial set of $\mathbf{s}_i$ values.

## 6.2 — A Simple Example

Suppose the organisms have a 1D trait space and use a common resource, $F$, so that the amount available per individual is

$$F_I = F \frac{b_0}{\int ds\ b(s)}$$

Growth will occur when $F_I > F_{crit}$ but saturates to a maximum value $g_m$ when the resources are plentiful. For example, we'll use

$$g = g_m \left( \frac{F_I - F_{crit}}{F_I} \right)_+$$

as in our discussion of the logistic equation; we end up with a similar system

$$\frac{\partial}{\partial t} b = (g - d)b + m \frac{\partial^2}{\partial s^2} gb \quad , \quad g = g_m \left( 1 - \frac{\langle b \rangle}{b_c} \right)_+$$

with $\langle b \rangle = \int ds\ b$. The coefficients $g_m$, $d$, and $b_c = Fb_0/F_{crit}$ are generally functions of $s$. The + subsript indicates application of the Heaviside function $(A)_+ = max(A, 0)$. The same form is obtained in an NP model assuming conservation among a dissolved nutrient pool and all of the phytoplankton, $N + \langle b \rangle = N_T$, with quadratic uptake

$$\frac{\partial}{\partial t} b = g_m \frac{N}{N_T} b - db = g_m \left( 1 - \frac{\langle b \rangle}{N_T} \right) b - db$$

For the logistic form, then, the growth rate

$$\mathcal{R}(s, E, b) = \mathcal{R}(s, b_c(s), b) = g_m(s) \left( 1 - \frac{\langle b \rangle}{b_c(s)} \right)_+ - d(s) \tag{6.3}$$

has a relatively simple structure. The environment here is the density of competitors for the resource as well as the value of $F$ or $N_T$ implicit in the carrying capacity.

Here the functional of $b(\mathbf{s})$ is the simplest one, $\langle b \rangle$, the integral of $b$. In later examples, we will have kernels with structure; e.g. if the competition is local we might have something like

$$\mathcal{R}(s, b) = g_m(s) \left( 1 - \frac{1}{b_c(s)} \int ds' e^{-\frac{1}{2}(s-s')^2/w_s^2}\ b(s') \right)_+ - d(s) \tag{6.4}$$

### 6.2.1 — Quota model

While the traits determine the vital rates, and thereby the fitness, the constraints or trade-offs organisms must make are equally important. Even a single-celled organism has specialized pieces it can use for transporting nutrients across the cell membrane, or pieces for using light energy, or ones which make swimming possible. The amount of cellular material allocated for the different functions will determine the rate at which it can grow and divide in a particular environment. (Organisms can adapt to different conditions and change the allocation of material, but we shall not deal with that.) As an analogy consider an oversimplified view of the oil industry. If all its equipment is intended for extracting oil and none for refining it, the income will be zero. Likewise, if all the equipment is for refining, the industry cannot survive. Some effort must be assigned to each of the functions to get income; with profit maximized for a particular division of effort. Furthermore, since the initial investors have provided finite funding, the industry cannot just increase the rates of extraction and refinement without bound.

These kinds of trade-offs and limitations apply in the case of organisms; they cannot simply increase their growth rate without bound, and different species allocate their machinery differently and are optimized for different environmental conditions. We shall use a version of Droop's(19xx) quota model to illustrate tradeoffs and the now indirect relationship between the trait variable $s$ and the growth rate $g_m$.

Droop proposed a two-stage model in which the required resources are taken into the cell to make up the "cell quota" $Q$; the production of new cells then depends on the ratio of this quota to the minimum requirements $Q_m$

$$\text{Div. rate} \propto \left(1 - \frac{Q_m}{Q}\right)_+$$

In the case of multiple required resources, this becomes

$$\text{Div. rate} \propto \min\left(1 - \frac{Q_{m,j}}{Q_j}\right)_+$$

giving a division rate (e-folding)

$$\mu = \mu_\infty(\mathbf{s}) \min\left(1 - \frac{Q_{m,j}(\mathbf{s})}{Q_j(\mathbf{s},t)}\right)_+ \tag{6.5}$$

with $\mu_\infty(\mathbf{s})$ describing the effects on reproduction of the trade-offs in various parts of trait space. With this form, the population numbers $n(\mathbf{s},t)$ grow according to

$$\frac{\partial}{\partial t} n = \left[\mu - d(\mathbf{s})\right] n \tag{6.6}$$

The cell quota increases by uptake of resources, with a saturating function, and decreases as the cells divide. Using the Monod form for uptake gives

$$\frac{\partial}{\partial t} Q_j = V_j(\mathbf{s}) \frac{N_j}{N_J + N_{h,j}(\mathbf{s})} - \mu Q_j \tag{6.7}$$

The Droop formulation suggests using a normalized excess quota $Q' = (Q - Q_m)/Q_m$ while the uptake form can be usefully written with a normalized resource value $N' = N_j/N_{h,j}$. The growth rate then depends on $Q'/(1+Q')$ and the uptake on $N'/(1+N')$. In addition to clarifying which parameters govern the behavior, the manipulations carry along fewer constants. However, it is not really necessary, so we shall leave the more familiar forms.

If the quota equations are in quasi-equlibrium

$$V_j \frac{N_j}{N_j + N_{h,j}} = \mu Q_j$$

The limiting resource will have the smallest l.h.s. as well; for this one, (indicated by 0 subscript)

$$V_0 \frac{N_0}{N_0 + N_{h,0}} = \mu Q_0 = \mu_\infty (Q_0 - Q_{m,0})$$

so that the growth rate also has a Monod form

$$\mu = \mu_\infty \frac{Q_0 - Q_{m,0}}{Q_0} = \mu_\infty \frac{v N_0}{(v+1)N_0 + N_{h,0}} \tag{6.8}$$

with $v_0 = V_0/Q_{m,0}\mu_\infty$ measuring the growth time compared to the time to increase the internal resource quota by $Q_{m,0}$. In terms of the populations, the specific growth rate is $UN/(N+K)$ with

$$U = \mu_\infty \frac{v_0}{1+v_0} \quad , \quad K = \frac{N_{h,0}}{1+v_0}$$

To explore trade-offs, we use two resources, nutrients ($N$) and light ($I$), with both excess nutrient and stored energy being required for growth. The growth rate will depend on the minimum of $q_N$ and $q_I$. In essence, we can calculate the growth rates for each resource separately using 6.8 assuming the others are not limiting; the actual growth rate will be the minimum of these. To express the advantages or disadvantages of increased ability to take in nutrients or light, we postulate that some amount of cell surface can be allocated for transporters which bring in nutrients or for chloroplasts but not both. If $s$ is the fraction of that area devoted to light-gathering,

$$v_N = (1-s)\hat{v}_N \quad \text{and} \quad v_I = s\hat{v}_I$$

(The trade-offs do not affect the maximum division rate $\mu_\infty$.) For fixed $N$ and $I$, the equilibrium $q_N$ and $q_I$ will have the same $(1-s)$ and $s$ factors. So the growth rate when light is limiting looks like

$$\mu = \mu_\infty \frac{s\,\hat{v}_I N_I}{N_I + N_{h,I} + s\,\hat{v}_I N_I}$$

and has a Monod shape as $s$ varies. Likewise, $\mu$, when $N$ is limiting, has a similar form in the variable $1-s$. The growth rate as a function of $s$ is the smaller of two Monod curves, one for energy extending up to the right and one for nutrients extending up to the left (figure 6.2). As the light decreases, the peak in growth rate decreases and moves

towards larger $s$ – the cells need more light-gathering machinery. Likewise, an increase in $N$ also moves the peak towards larger $s$, since they can take up enough nutrients with fewer transporters and can increase their growth by increasing the number of photoreceptors.

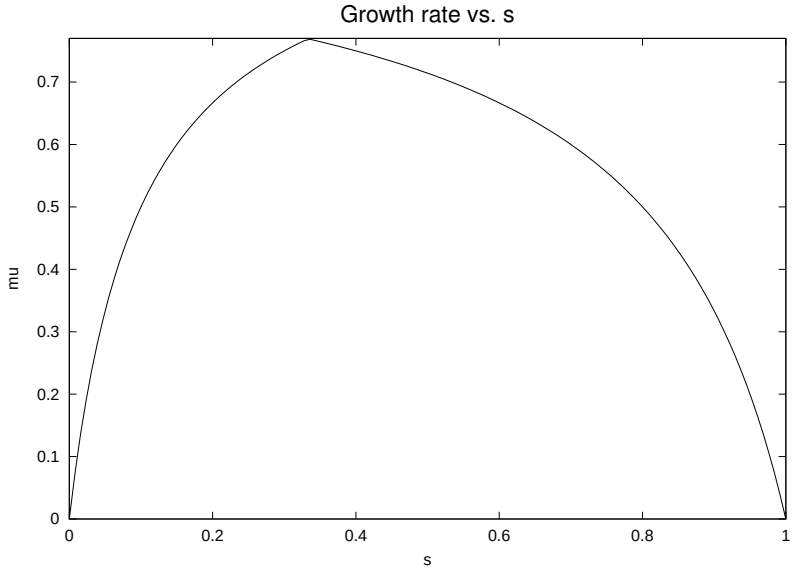


Figure 6.2: Division rate $\gamma/\mu$ vs. $s$ for $U_N = 5$ and $U_I = 10$.

For analytical convenience, we use a smooth form

$$\mu = \mu_m 4s(1-s)$$

### 6.2.2 — Quota model for predators

We can also view predation as a two-step process, leading to a Monod form. We consider the intake of food as proportional to the concentration and the empty volume in the gut. This could come about, for example by selecting only the smaller and smaller prey fraction as there is less and less room in the gut. Then the effective available food is roughly proportional to the total concentration $F$ over all sizes times the empty gut volume. As food is processed, the gut empties and the biomass grows:

$$\frac{\partial}{\partial t}G = \gamma F(G_{max} - G) - \lambda G$$
$$\frac{\partial}{\partial t}b = \lambda G b - \dots$$

If the gut is in equilibrium,

$$G = \frac{\gamma F G_{max}}{\gamma F + \lambda}$$

and

$$\frac{\partial}{\partial t}b = \lambda G_{max}\frac{F}{F + \lambda/\gamma}b - \dots \tag{6.9}$$

For tradeoffs, we can take $s$ to be the ratio of $G_{max}$ to the animal's volume, $\lambda$ to be proportional to the gut surface area $s^{2/3}$, and the abililty to gather food, $\gamma$, proportional to the non-gut volume, $1-s$. Then we again get a growth rate curve (now smooth) which vanishes at $s=0$ and $s=1$ and which has an intermediate maximum

$$\lambda_0 G_0 s^{5/3} \frac{F}{F + (\lambda_0 s^{2/3}/\gamma_0[1-s])}$$

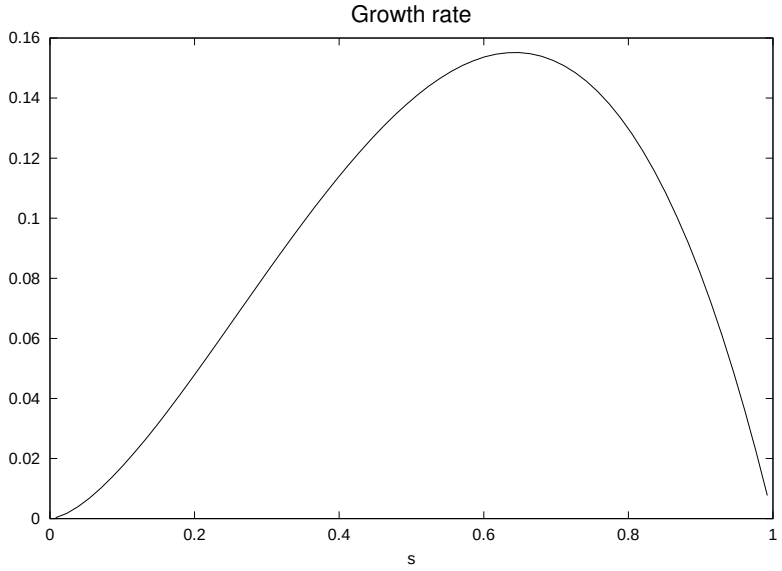


Figure 6.3: Growth rate (divided by $\lambda_0 G_0$) vs. $s$ for $F\gamma_0/\lambda_0 = 1$.

### 6.2.3 — Evolutionarily Stable Strategies

Consider first the problem without advection or diffusion. When $m = 0$, we have many possible singular solutions of the form

$$b(s,t) = \overline{b}(t)\delta(s-\overline{s})$$

with $\overline{b}$ satisfying

$$\frac{\partial}{\partial t}\overline{b} = \mathcal{R}(\overline{s},\overline{b})\,\overline{b}$$

since $E = \langle b \rangle = \overline{b}$. In our case, this is just the the logistic equation and steady solutions $\mathcal{R}(\overline{s}|\overline{b}) = 0$ have

$$\overline{b} \to b_c(\overline{s})\ \frac{g_m(\overline{s}) - d(\overline{s})}{g_m(\overline{s})}$$

Let us introduce a different organism with phenotype $s'$: $b = \overline{b}(t)\delta(s-\overline{s}) + b'(t)\delta(s-s')$; if its biomass is very low, it satisfies

$$\frac{1}{b'}\frac{\partial}{\partial t}b' = \mathcal{R}(s'|\overline{b}) = \left[g_m(s')\left(1 - \frac{\overline{b}}{b_c(s')}\right) - d(s')\right]$$

When the coefficients are time-independent, we can write this in the simpler form

$$\frac{1}{b'}\frac{\partial}{\partial t}b' = \frac{g_m(s')}{b_c(s')}\left[\frac{g_m(s')-d(s')}{g_m(s')}b_c(s') - \frac{g_m(\overline{s})-d(\overline{s})}{g_m(\overline{s})}b_c(\overline{s})\right] = g_m(s')\frac{\overline{b}(s')-\overline{b}(\overline{s})}{b_c(s')}$$

where $\overline{b}(s')$ is the equilibrium population for $s = s'$. The population with the largest value of $\overline{b}(s)$ will exclude all others. (This is by no means a general result.) Alternatively, this populaion is the one which reduces the available nutrient the most, minimizing $F_I$. The idea (Tilman, 19xx) that the ESS is the one which survives on the minimal resource level and drives the resource down below the value the others require will appear in more complex problems as well.

Figure 6.4 illustrates the process, taking $g_m = 4s(1-s)$; we begin with a random $b(s)$ such that $\mathcal{R}$ is positive in some range. These grow and reduce the value of $\mathcal{R}$ until only the plankton near the maximum can continue to thrive. Then the slow process of excluding the neighbors with very slightly negative $\mathcal{R}$ values continues, with $b(\overline{s})$ increasing as the width narrows, tending towards a delta function (or proportional to $1/ds$ in the numerical implementation). This case illustrates the "sharing' of a delta function at $s = 0.5$ among two neighboring grid points; by the symmetry in the location of these at $\frac{1}{2} \pm \frac{1}{2}ds$, the values reach a limit such that their sum is $(b_c/ds)\left[1 - d/g_m(\frac{1}{2} \pm \frac{1}{2}ds)\right]$.

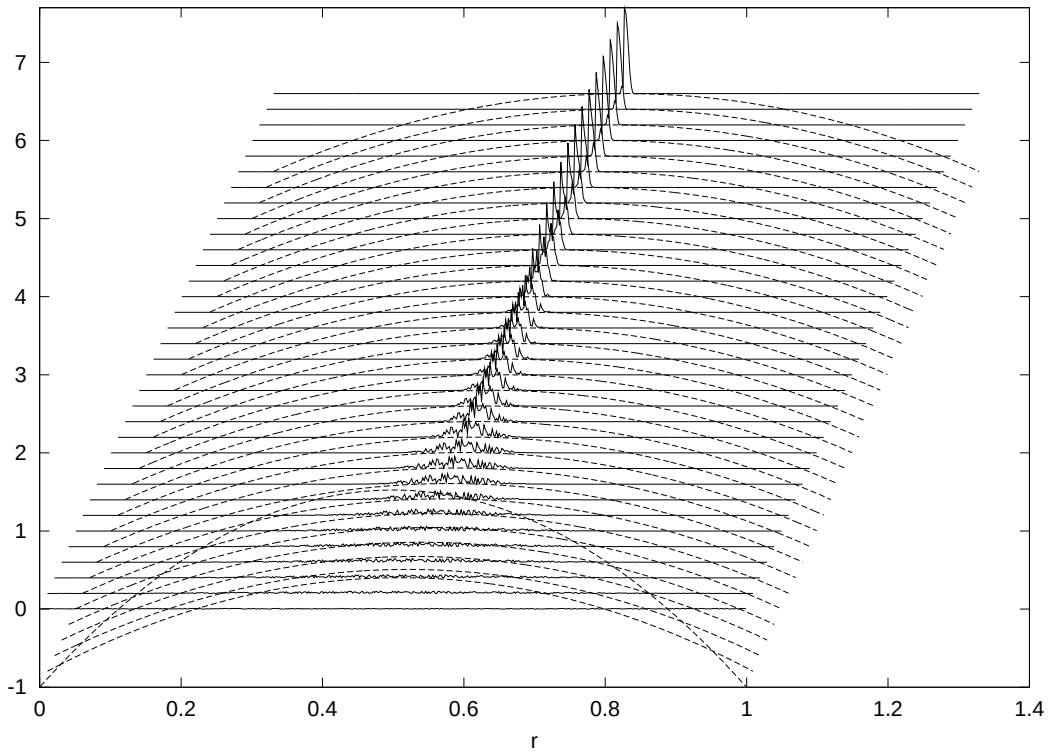


Figure 6.4: $b$ and $5\times\mathcal{R}$ at $t$ =[0:10:50, 100:100:500, 1000:500:4500, 5000:5000:75000] with each profile offset upwards and to the right.

Another illuminating example comes from starting with a population centered around a non-optimal value (figure 6.5). $\mathcal{R}$ again decreases rapidly as the population grows;

however, for short times it now approaches a state where it is nearly zero averaged over the group but has a noticeable slope so that the ones closer to the ESS are growing and the ones further away are decaying. On longer times, this generates a drift towards the ESS. As we shall see below, the rate of drift depends on the pulse width, so that in the absence of mutation it slows dramatically.

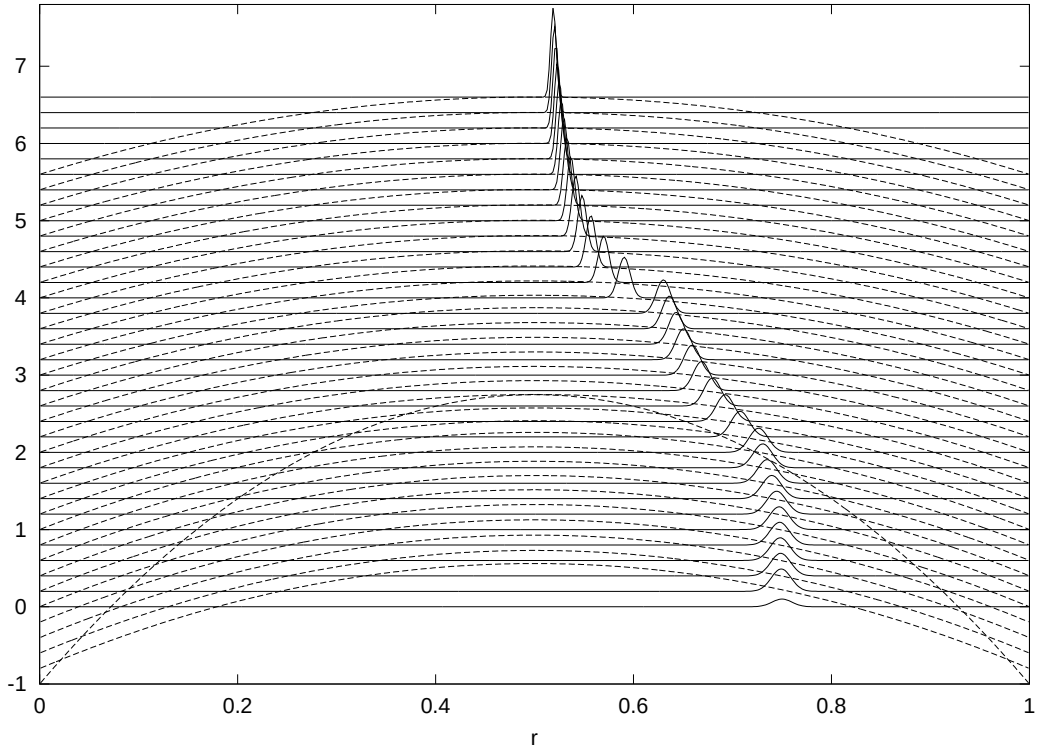


Figure 6.5: like the previous figure but with a different starting condition. Profiles are not offset to the right here.

### 6.2.4 — Local case

Competition is usually local in space, but it can also be local in time or in trait-space. For example, if the trait $s$ is related to weight (or log weight), the resources (prey) for organisms with widely different $s$ values will generally not utilize the same $F$, whereas rather similar organisms will overlap in the food supply. We adopt the form

$$\mathcal{R}(s|b) = g_m(s)\left(1 - \frac{1}{b_c(s)}\int ds' G(s-s')b(s')\right) - d(s)$$

with $d$ and $b_c$ constant, $G$ gaussian (as in 6.4) with width $w_s = 0.1$, and $g_m$ quadratic as before, and we start with a broad, off-center population. It quickly settles, but now the growth rates at small $r$ are not suppressed as the original population equilibrates. As a result, new phenotypes branch off and move towards the peak $\mathcal{R}$ values until an equilibrium with 6 species appears. At longer times, the peaks will narrow and steepen, keeping the same biomass, with the long-time state having 6 delta functions (again spread

numerically). Note the evens in which one rather spread out peak splits into two distinct types.

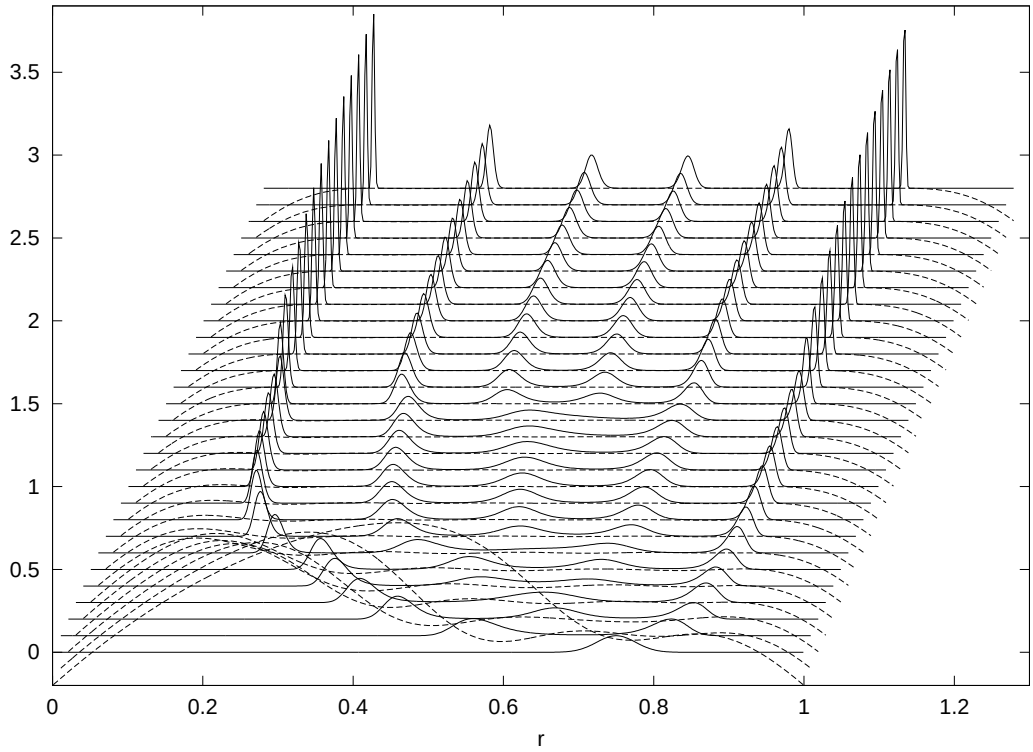


Figure 6.6: Local competition.

The solution here satisfies the Fredholm integral equation of the first kind

$$\int_{s_0}^{s_1} G(s-s')b(s') = b_c(s)\left[1 - \frac{d(s)}{g_m(s)}\right]$$

For the singular solutions $b = b_i\delta(s - s_i)$, this turns into a matrix equation; we can search for the set of $s_i$ values such that all the $b_i$'s are positive and $\mathcal{R} \leq 0$ over the domain. We can also use the techniques of adaptive dynamics (below) to find singular solutions.

As the competition becomes more and more local ($w_s$ smaller), the solution has more peaks until, in the delta function limit when each organism competes only with others of exactly the same type, $b$ becomes continuous and equal to the right-hand side of the equation above. Interestingly, cusped kernels such as $G = \exp(-|s - s'|/w_s)$ also have continuous solutions. Such a form seems less reasonable, since we would expect a smooth peak for competition; however, this is the structure of the correlation function for a first-order autoregressive process, so it could be relevant for a different problem. In any case, it does indicate the sensitivity of this kind of problem to assumptions about the kernel.

### 6.2.5 — Time-dependence

For time-dependent problems, we can take a time-average to find

$$\frac{1}{T}\ln\frac{b'(T)}{b'(0)} = \langle \mathcal{R}(s',t|\overline{b}(\overline{s},t)\rangle \equiv R(s'|\overline{s})$$

Then $\overline{s}$ will represent an ESS if

$$R(\overline{s}|\overline{s}) = 0 \quad \text{[definition]} \qquad \text{and} \qquad R(s'|\overline{s}) < 0 \quad \text{for} \quad s' \neq \overline{s}$$

Organisms with a non-optimal phenotype will die out. Locally, these conditions become

$$\frac{\partial}{\partial s'}R(s'|\overline{s})\big|_{s'=\overline{s}} = 0 \quad , \qquad \frac{\partial^2}{\partial s'^2}R(s'|\overline{s})\big|_{s'=\overline{s}} < 0$$

For the logistic-type model with periodic forcing, we can evaluate $R(s'|\overline{s})$ as follows: given $\overline{s}$ we find the periodic solution $\overline{b}(\overline{s},t)$ by writing the equation in terms of $1/b$. We can then integrate

$$\frac{\partial}{\partial t}\overline{b} = \mathcal{R}(\overline{s}|\overline{b})\overline{b}$$
$$\frac{\partial}{\partial t}\hat{R}(s',t) = \frac{1}{T}\mathcal{R}(s'|\overline{b})$$

over a period $T$ with the final value being $R(s'|\overline{s}) = \hat{R}(s',T)$. As an example, we let the point of maximum growth with respect to $s$ to migtrate back and forth over the season as well as adding a modulation in its amplitude (figure 6.7).

$$g_m = 24(1-\delta_g\cos(\omega t))[r-\delta_r\cos(\omega t)][1-r+\delta_r\cos(\omega t)] - 5$$

when positive.

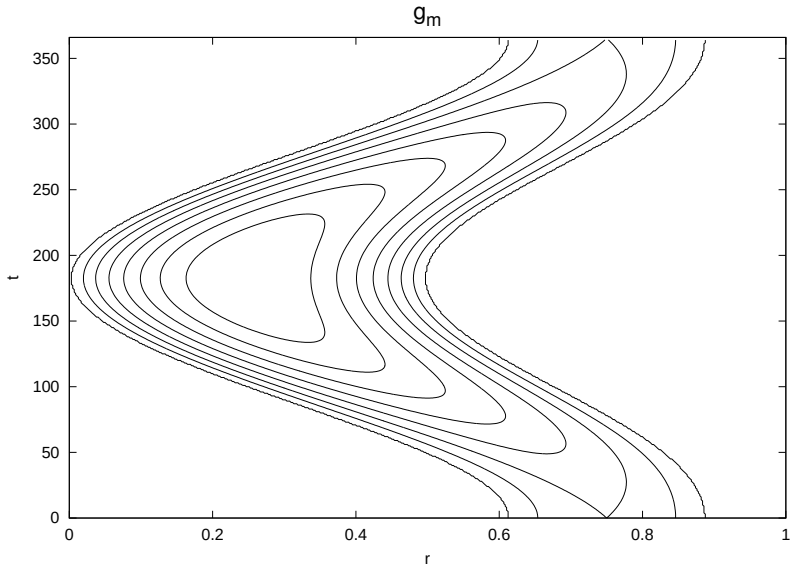

Figure 6.7: $g_m(r,t)$ with contours from 0 to 1.4 with $\delta_g = 0.1$ and $\delta_r = 0.25$.

When we look at $R(s', \overline{s})$, it turns out to have local ESS conditions for two values of $\overline{s}$, but neither is globally stable (see example in figure 6.8). Instead, the global ESS (figure 6.9a) has two separate species, one optimized for summer, and the other for winter (which peaks in late winter because it has to recover from very low values) (figure 6.9b).

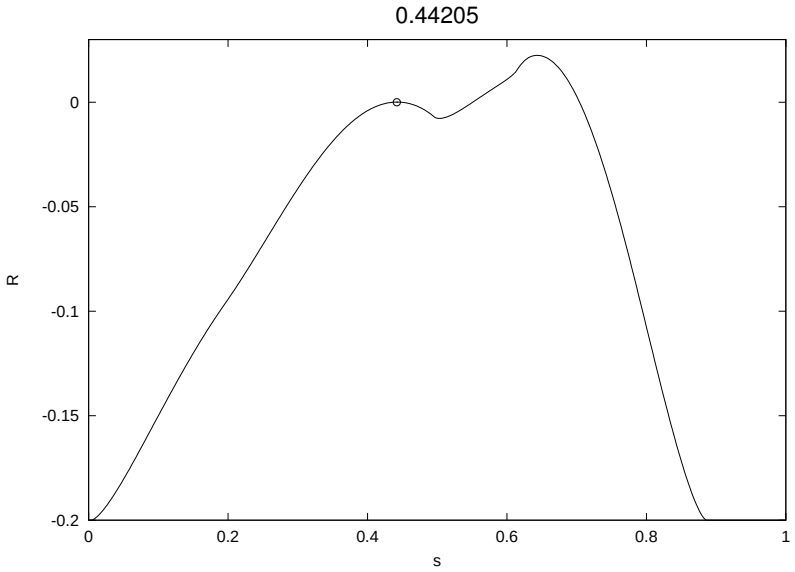


Figure 6.8: $R(s|\overline{s})$ for one of the local ESS states.

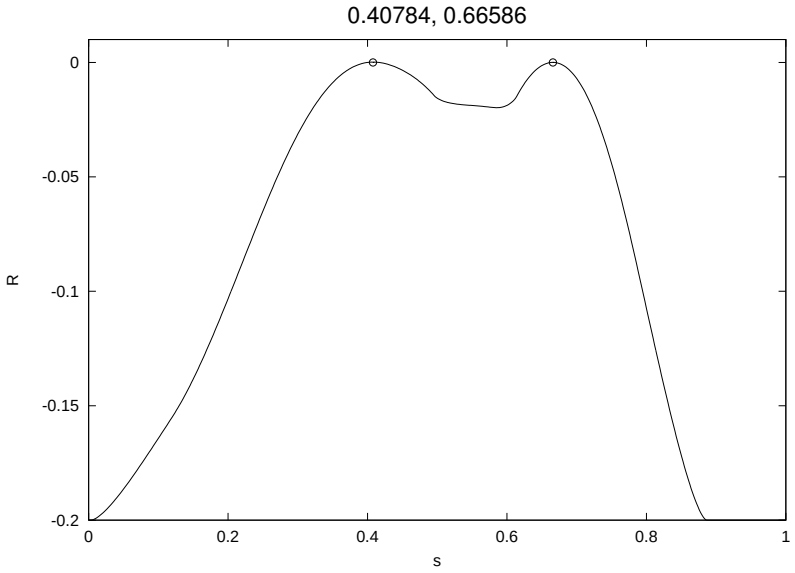


Figure 6.9a: $R(s|\overline{s})$ for the global ESS state.

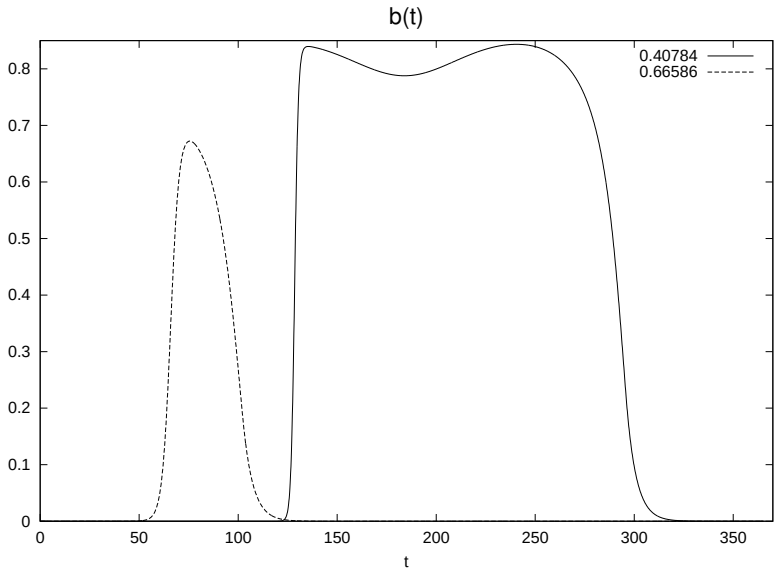


Figure 6.9b: $\overline{b}(t)$ for the global ESS.

Seasonal succession is sometimes ascribed to "temporal niches" associated with different $s$ values being dominant at different times of the year if the conditions remained steady. This example has that character; however, we shall see that it seems less likely when the growth rate variations depend on light and nutrients.

### 6.2.6 — With mutation

When $m$ is not zero, we can still look for steady solutions

$$m\frac{\partial^2}{\partial s^2}gb = db - gb = \left[\frac{d}{g} - 1\right] gb$$

This is a form of Schröedinger's equation with $d/g$ playing the role of the potential; a local maximum in $g$ results in a potential well, and we can find "bound states" with localized solutions for $gb$. Indeed, if $g = g_0/(1 + \frac{1}{2}\alpha(s - s_0)^2)$ with $g_0 = g_m(1 - \langle b\rangle/b_c)$, $gb$ will have a Gaussian form

$$gb = A\exp(-\frac{1}{2}(s - s_0)^2/w^2)$$

with $w^2 = \frac{1}{2}[\sqrt{m^2 + 8m\alpha}+m]$. The solution requires a particular value of $g_0 = \frac{d}{4}[\sqrt{\alpha^2m^2 + 8\alpha m}+ \alpha m + 4]$ which then determines the population level $A$.

### 6.2.7 — Relationship to stability theory

To understand the relationship to stability theory, look again at the linearized model

$$\frac{\partial}{\partial t}b' = \mathcal{R}(s|\overline{b})b' + \overline{b}\frac{\partial \mathcal{R}}{\partial E}\langle b'\rangle$$

with the basic state having

$$\overline{b}(s)\mathcal{R}(s|\overline{b}(s)) = 0$$

For standard problems, the mean state is non-zero $\overline{b}(s) \neq 0 \Rightarrow \mathcal{R}(s, \overline{b}(s)) = 0$, the first term vanishes, and we deal only with the second term. For multiple species, this would become

$$\frac{\partial}{\partial t}b'_i = \overline{b}_i \frac{\partial \mathcal{R}_i}{\partial b_j}\Big|_{b=\overline{b}} b'_j$$

as in chapter xx.xx.

In the case of an ESS, $\overline{b}(s) = 0$ for $s \neq \overline{s}$ so that $\mathcal{R}(s|\overline{b}) \neq 0$ and the first term is the important one. This case seems less familiar, but is similar to showing that a state with only $N$ and $P$ will be unstable to adding $Z$. Likewise in the weight-structure models, we have seen that the analogues to both terms must be included (xx.xx).

In the case with mutation, the base solution is non-zero everywhere

$$\overline{b}\mathcal{R}(s|\overline{b}) + \nabla_s m \nabla_s \, g(s|\overline{b})\overline{b} = 0$$

and the perturbation equations

$$\frac{\partial}{\partial t}b' = \mathcal{R}(s|\overline{b})b' + \overline{b}\frac{\partial \mathcal{R}}{\partial E}\langle b'\rangle + \nabla_s m \nabla_s \, b'$$

clearly have both terms entering. Near the "hotspots" where $\overline{b}$ is large, $\mathcal{R}$ is relatively small, the second term dominates, and the problem looks like a standard stability system modified by diffusion. Far away, however, $\overline{b}$ is small, and the basic state has a decaying form with $\mathcal{R}$ nonzero. If $\mathcal{R}$ changes and becomes positive in that region, the population can "tunnel" into the local maximum and grow. The amount of time this will take depends on distance and the mutation rate.

### 6.2.8 — Mixing

To analyze the effects of mixing on this kind of system, we consider a system with diffusion and spatially variable properties favoring different $s$ values at different latitudes

$$\frac{\partial}{\partial t}b = b\mathcal{R}(s, \mathbf{x}|\langle b\rangle) + \nabla\kappa\nabla b + \frac{\partial}{\partial s}\mu\frac{\partial}{\partial s}b$$

Figure 6.10 shows an example solution for the $\mathcal{R}(s, y|0)$ pictured with

$$g_m = [24(1 - s + s_0)(s - s_0) - 5](1.4 - 0.8y/L) \quad , \quad s_0 = -0.25\cos(\pi y/L)$$

The population has isolated, overlapping bands, with each band having a sharp peak at a particular $s$ value and extending over a limited spatial range.

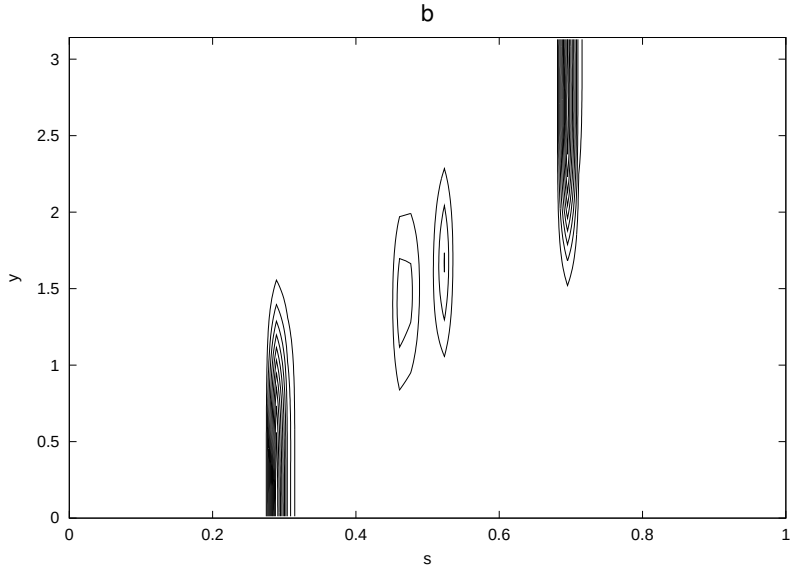


Figure 6.10: Contours of $b(s, y)$ with $\kappa = 0.01$.

To understand this solution, consider the case neglecting mutation. We can find single-species solutions $b = \overline{b}\,\delta(s - \overline{s})$ satisfying

$$\frac{\partial}{\partial t}\overline{b} = \overline{b}\mathcal{R}(\overline{s}, \mathbf{x}|\overline{b}) + \nabla\kappa\nabla\overline{b} \tag{6.10}$$

This type can develop from a seed population if the eigenvalue $\sigma_0$ from

$$\sigma_0 b_0 = b_0\mathcal{R}(s, \mathbf{x}|0) + \nabla\kappa\nabla b_0 \tag{6.11}$$

is positive. This is a form of Schrödinger's equation, with $-\mathcal{R}$ playing the role of a potential; "bound states" correspond to growing solutions, although we are only interested in the gravest mode which has $b_0$ everwhere positive. Such states can exist if the region

where $\mathcal{R}(\overline{s}, y|0) > 0$ is big enough and strong enough to overcome diffusive losses into the region where the death rate dominates (Kierstead and Slobodkin)

$$growth \times L^2 > \kappa$$

Likewise in regions where the population is dying, it will decay over a scale

$$L_{decay} \sim \sqrt{\kappa/d}$$

If the growth rates are small, we can estimate the final state amplitude and structure by multiplying eqn. 6.10 by $b_0$, subtracting $\overline{b}$ times 6.1, and integrating over space. Assuming boundary fluxes vanish leads to

$$\frac{\partial}{\partial t}\int \overline{b}b_0 = \sigma_0 \int \overline{b}b_0 - \int \overline{b}b_0 \Big[\mathcal{R}(\mathbf{x}, \overline{s}|0) - \mathcal{R}(\mathbf{x}, \overline{s}|\overline{b})\Big]$$

Now we add the assumption of small growth rate implying the amplitude is also small and the structure is close to the eigenfunction $b_0$ so that $\overline{b} \simeq \alpha(t) b_0$. Then $\alpha$ satifies the logistic equation

$$\frac{\partial}{\partial t}\alpha = \sigma_0 \alpha - \gamma \alpha^2$$

with

$$\gamma = \int b_0^2 \left[-\frac{\delta \mathcal{R}}{\delta \overline{b}} b_0\right] \Big/ \int b_0^2$$

allowing us to estimate the population amplitude. When the growth rates are larger, we can still solve 6.10 numerically to find the equilibrated $\overline{b}(y)$.

Perturbations at a different point $s'$ in trait space will grow if the eigenvalue problem

$$\sigma(s')b' = \mathcal{R}(s', \mathbf{x}|\overline{b})b' + \nabla \kappa \nabla b' \tag{6.12}$$

has a solution with the real part of $\sigma(s')$ positive. If $\delta s \equiv s' - \overline{s}$ is small, the solution will be $b' = \overline{b} + \hat{b}\,\delta s$ with

$$\sigma \overline{b} \simeq \mathcal{R}(\overline{s}, \mathbf{x}|\overline{b})\hat{b} + \nabla \kappa \nabla \hat{b} + \frac{\partial \mathcal{R}}{\partial s}\overline{b} \tag{6.13}$$

Using the self-adjoint property of 6.12-13, we find

$$\sigma(\overline{s} + \delta s) \simeq \delta s \int d\mathbf{x} \frac{\partial \mathcal{R}}{\partial s}\overline{b}^2 \Big/ \int d\mathbf{x}\, \overline{b}^2$$

so that a local ESS will satisfy

$$\int d\mathbf{x} \frac{\partial \mathcal{R}}{\partial s}\overline{b}^2 = 0$$

In the small growth rate case, this occurs when the growth rate from 6.10 is maximal, but this is not a general result. As in the zero-dimensional case, the ESS still represents the point at which the available nutrient is insufficient for plankton with any other trait value.

The situation is more complex, because the nutrient is reduced differently at different spatial locations. Other traits may be favored at other points in the domain, but cannot offset the diffusive losses.

As the growth rate increases, or the death rate decreases, the trait corresponding to a local ESS cannot suppress growth at a more distant $s$ value. We can show this by comparing $\sigma_0$ with $\sigma$ (figure 6.11). When the positive $\sigma$ region appears, we expect to find a new solution with both traits appearing. Each one has peak populations where the local growth rate is maximal, but they extend into the other region because of the diffusion.

Figure 6.11: xx

The example in figures 6.10-11 has a simple growth rate pattern

$$\mathcal{R} = \left[R_0 - \frac{1}{2}R_2(s - s_0(y))^2\right]_+ \left[1 - \frac{\langle b\rangle}{b_c}\right] - d$$

with

$$s_0 = \left[\frac{1}{2} - \delta_s \cos(\pi y/L)\right]\left[1 - \delta_y(y - L/2)\right]$$

By varying $d$, we can see the successive appearence of different groups, each having a "home region" in which it can grow well with the other groups having only a small damping effect because they are only sustained by diffusive input balancing the death rate; i.e., they are multiple decay lengths $L_{decay}$ from the region of growth . This shows up when we plot the population of each type against its growth rate (figure 6.12).

Figure 6.12: xx

### 6.2.9 — Advection

If we have a steady circulation, the parcels moving on each streamline encounter time-dependent forcing. As an example, we take the Stommel circulation model, which has a rapid western boundary current ($1m/s$ with width $\ell = 75\,m$ in a $L = 5000\,km$ square box. The streamfunction (to a reasonable approximation when $\ell << L$) is

$$\psi = V_0\ell\,[1 - x/L - \exp(-x/l)]\sin(\pi y/L)$$

Circulation times range from a few years for parcels staying near the western boundary to a decade for those passing near the center of the box and several decades for those closer to the outer edges. We assume that $\mathcal{R}$ varies with $y$ in the same way as above (figure 6.13).

Because the time scales are long, nothing can survive on the outer trajectories; all types are subjected to prolonged periods during which they are unable to grow. On the innermost trajectories, conditions do not change much, so a dominant type becomes established, close to that which would exist at the central latitude in the absence of motion. Further out, we have a few trajectories with low $s$ values in the inflow and the western boundary current, a transition to an intermediate type in the outflow, a high value ocean interior which then steps down in low latitudes.

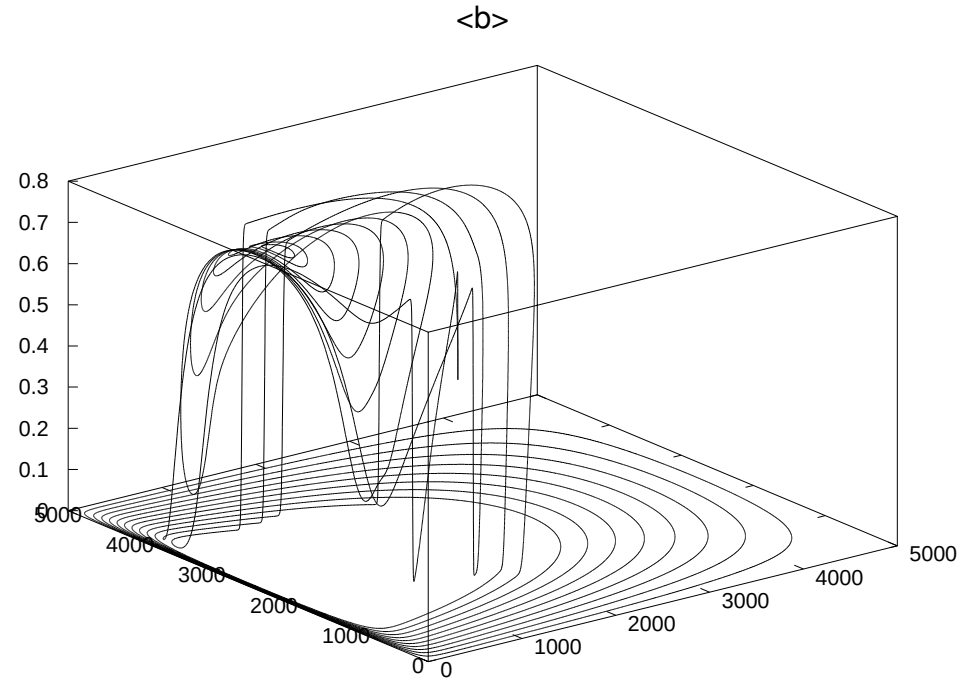


Figure 6.13a: Values of $\langle b \rangle$ along streamlines.

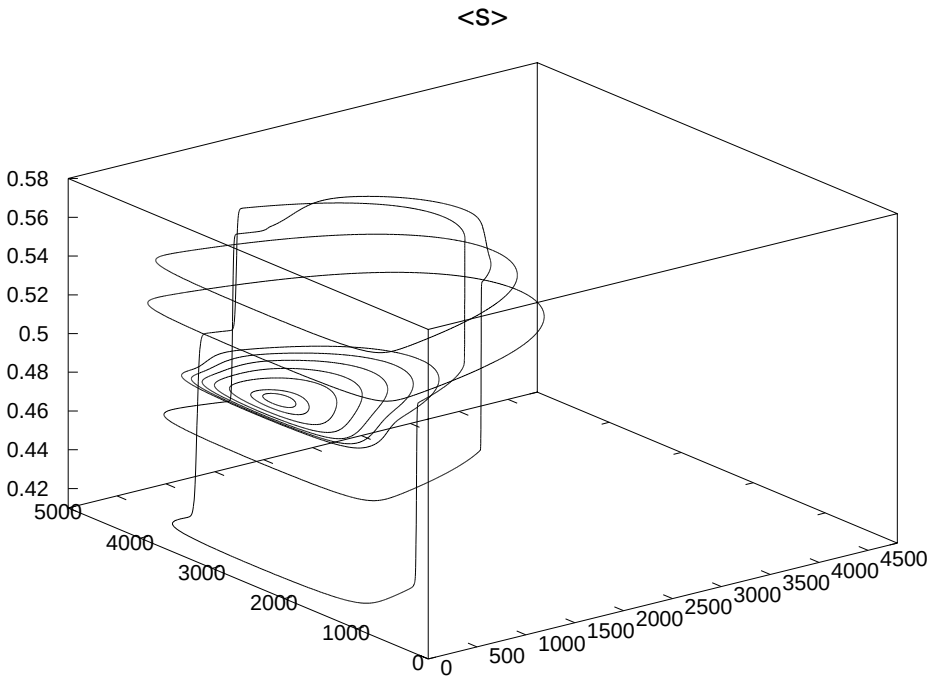


Figure 6.13b: Values of $\langle sb \rangle / \langle b \rangle$ along streamlines.

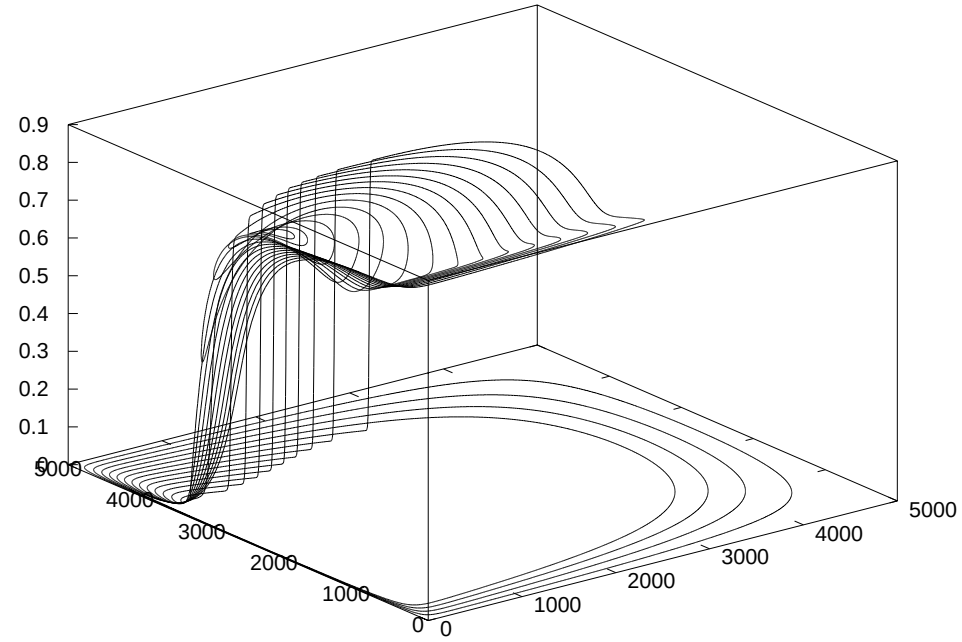


Figure 6.14a: Values of $\langle b \rangle$ along streamlines for $\mu = 10^{-9}$.

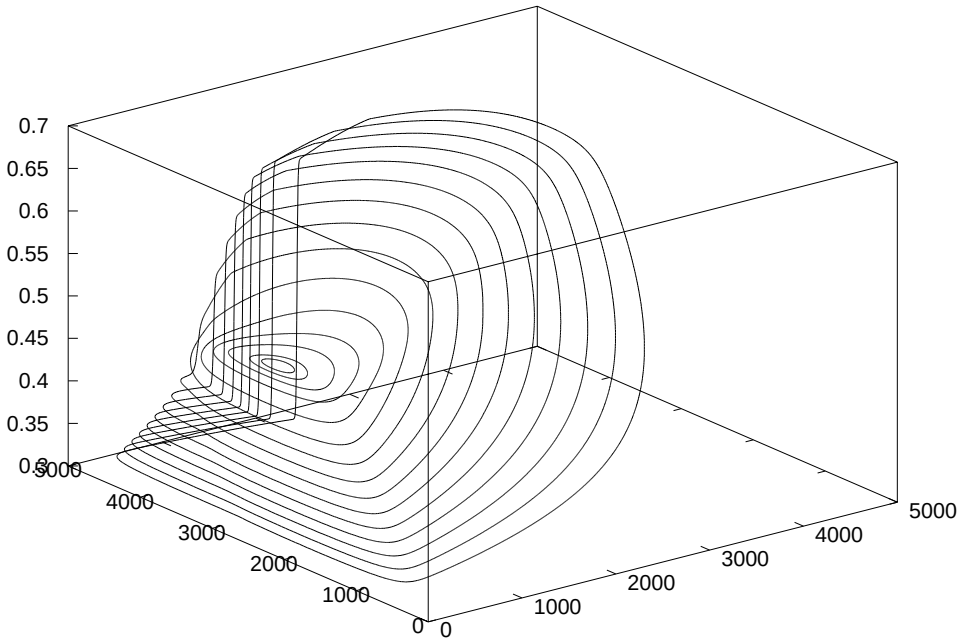


Figure 6.14b: Values of $\langle sb \rangle / \langle b \rangle$ along streamlines.

With a small spreading/ mutation rate ($10^{-9}$ $d^{-1}$), the transitions smooth out (figure 6.14). We still see low $s$ types in the western boundary current with a drop in the biomass; these both recover in the outflow region.

If we include both advection diffusion, using a 2D numerical code with the same Stommel circulation, we find much of the domain is dominated by diffusion, some of it numerical.

Figure 6.15: xx

## 6.3 — More general cases

The previous section used a simple example to illustrate the main principles; now we need to examine some of the complications which arise even in a model having only autotrophs. If the PP rely on a single nutrient

$$\frac{\partial}{\partial t} b = \mathcal{R}(s, N) b$$

we can see that a local ESS will also be an extremum for $N$. The singular solution has $b = \overline{b}(\overline{s})\delta(s - \overline{s})$. The nutrient level will be adjusted to $\overline{N}(\overline{s})$ such that $\mathcal{R}(\overline{s}, \overline{N}) = 0$. Taking a first derivative gives

$$\frac{\partial \mathcal{R}}{\partial \overline{s}} + \frac{\partial \mathcal{R}}{\partial N} \frac{\partial \overline{N}}{\partial \overline{s}} = 0$$

For a local ESS, the first term vanishes; since $\mathcal{R}$ is most likely monotonically increasing with $N$, we see that $\overline{N}(s)$ has an extremum also. The second derivative at the critical point

$$\frac{\partial^2 \mathcal{R}}{\partial \overline{s}^2} + \frac{\partial \mathcal{R}}{\partial N} \frac{\partial^2 \overline{N}}{\partial \overline{s}^2} = 0$$

implies a local maximum or $\mathcal{R}$ with repsect to $s$ will be a local minimum in $\overline{N}(s)$ as Tilman(19xx) argues.

Expressing the conditions

$$\mathcal{R}(\mathbf{s}', \overline{N}_i, \overline{b}) \leq 0$$

(with the zero obtained only for $\mathbf{s} = \overline{\mathbf{s}}$) can also be done explicitly in terms of the vital rates. For example,

$$\mathcal{R} = \mu(s) \frac{N}{N + N_h(s)} - d(s)$$

has the steady resource level

$$\overline{N} = \frac{\overline{d}\, \overline{N}_h}{\overline{\mu} - \overline{d}}$$

with the overbars indicating evaluation at $s = \overline{s}$. The ESS condition

$$\mu \overline{N} \leq d N_h + d \overline{N}$$

implies

$$\frac{\mu - d}{d N_h} \leq \frac{1}{\overline{N}} = \frac{\overline{\mu} - \overline{d}}{\overline{d}\, \overline{N}_h} \tag{6.14}$$

Thus the ESS occurs at the $s$ which maximizes $(\mu - d)/dN_h$ (and not in general at the point where the growth rate $\mu$ is highest) and minimizes $\overline{N}$. In this case, the nutrient equation (e.g. a chemostat model with

$$\frac{\partial}{\partial t}N = -\int ds\mu(s)\frac{Nb(s)}{N + N_h(s)} + \lambda(\hat{N} - N)$$

where $\hat{N}$ is the nutrient level of the inflow) plays no role in the selection process; instead, it determines the population level

$$\overline{b} = \frac{\lambda}{d(\overline{s})}(\hat{N} - \overline{N})$$

Uptake/ assimilation trade-off

Klausmeier, *et al.*(20xx) suggest a trade-off in which cell machinery can be allocated either to nutrient uptake ($V_N = \hat{V}_N(1 - s)$) or the building of cell mass ($\mu_\infty = s\hat{\mu}_\infty$), giving $v_N = s\hat{v}_n/(1 - s)$. If the quota is in equilibrium, then the growth has the form $UN/(N + H)$ with the coefficients being

$$U = \frac{\mu V}{\mu Q_m + V} = \frac{\hat{\mu}_\infty s(1 - s)\hat{v}_N}{s + (1 - s)\hat{v}_N}$$

and

$$H = \frac{\mu Q_m}{\mu Q_m + V}N_h = \frac{N_h s}{s + (1 - s)\hat{v}_N}$$

The function we need to maximize

$$R(\mathbf{s}) = \frac{U - d}{Hd} = \frac{1}{N_h}\left[\frac{\mu - d}{\mu d}\frac{V}{Q_m} - 1\right] \tag{6.15}$$

has a peak – the ESS – at $\overline{s} = \sqrt{d/\hat{\mu}_\infty}$.

### Two required resources

When the organism has two required resources for growth or has alternatives, with trade-offs between the two, the optimal value of the trait parameter regulating this trade-off depends on the strength of the forcing (e.g., $\hat{N}_1$ and $\hat{N}_2$). If we use the same quota model and consider $d$ to be constant, the ESS will have both nutrients limiting simultaneously; otherwise the population $n$ will be centered on a region where $\mu$ is an increasing or decreasing function of $s$. The only point where it can settle thus has

$$\frac{Q_1}{Q_{m,1}} = \frac{Q_2}{Q_{m,2}} \tag{6.16}$$

The number equation

$$\frac{1}{n}\frac{\partial}{\partial t}n = \mu_\infty \min\left(1 - \frac{Q_{m,1}}{Q_1}\,,\, 1 - \frac{Q_{m,2}}{Q_2}\right) - d$$

implies

$$Q_j = Q_{m,j}\frac{\mu}{\mu - d}$$

The quota equations then give us the uptake rates

$$\frac{V_j N_j}{N_j + N_{h,j}} = Q_{m,j}\frac{\mu_\infty d}{\mu_\infty - d}$$

If the trait parameter $s$ sets the relative efficiency of uptake $V_1 \propto (1-s)$ and $V_2 \propto s$, these equations give $N_1$ and $N_2$ as M-functions of $s$. Using the uptake expressions in the ratio of the two (equilibrium) nutrient equations gives another expression

$$\frac{\hat{N}_1 - N_1(s)}{\hat{N}_2 - N_2(s)} = \frac{Q_{m,1}}{Q_{m,2}} \tag{6.17}$$

which will leads to a quadratic expression for $s$ with coefficients depending on $\hat{N}_1/Q_{m,1} - \hat{N}_2/Q_{m,2}$. Clearly, changing the inflow nutrient levels will change the value of $s$; the optimal type will depend upon the environmental conditions (Figure 6.16).

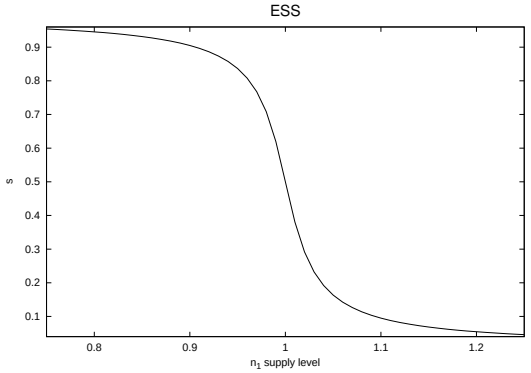


Figure 6.16: Predicted $s$ value in a simple case.

### Alternative resources

For another case, consider an organism which can use either of two resources, though they may different nutritional value. It can tradoff the effort to acquire one or the other; the food intake could be represented as

$$F = sR_1 + (1-s)\alpha R_2$$

with

$$\begin{aligned}
\frac{\partial}{\partial t} b &= \mu \frac{F}{F+F_0} b - db \\
\frac{\partial}{\partial t} R_1 &= -\mu R_1 \int \frac{sb}{F+F_0} + \lambda(\hat{R}_1 - R_1) \\
\frac{\partial}{\partial t} R_2 &= -\mu\alpha R_2 \int \frac{(1-s)b}{F+F_0} + \lambda(\hat{R}_2 - R_2)
\end{aligned}$$

For this problem, the resource values approach $R_1 = \alpha R_2 \equiv F_*$, in which case, $F$ becomes $F_* = dF_0/(\mu - d)$, independent of $s$, and we can have a continuous $b(s)$ solution (figure 6.17). The $b$ function is weakly constrained such that

$$\int sb = \frac{\lambda}{d}(\hat{R}_1 - F_*) \quad , \quad \int b = \frac{\lambda}{d}(\hat{R}_1 + \hat{R}_2 - \frac{\alpha+1}{\alpha} F_*) \quad ;$$

otherwise, the shape depends on the initial conditions. This is an example of Hubbell's "neutral evolution" having multiple coexisting types, none of which have a selective advantage over the others. If we start with a single type which equilibrates $b = \overline{b}\delta(s - \overline{s})$, with $\overline{s}$ given by the ratio of the two integrals above, $\overline{F} \to F_*$ becomes independent of $s$ so that the growth rates for all $s \neq \overline{s}$ are zero.

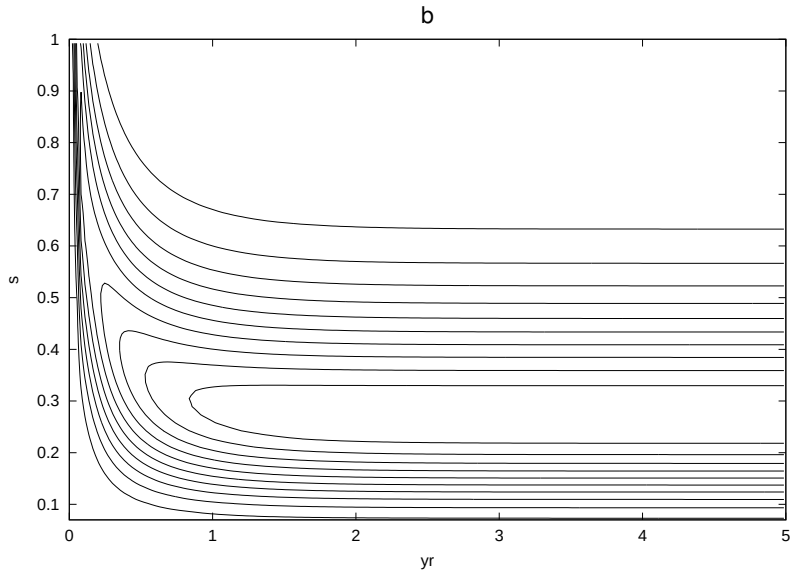


Figure 6.17: evolution of $b$ for the alternative resources model.

As in Barton, *et al.* (20xx), time-dependent forcing selects a single $s$ value. To see this, let us non-dimensionalize the equations, scaling time by $1/d$, $b$ and $F$ by $F_*$, $R_1$ by $R_{1*} = F_*$, and $R_2$ by $R_{2*} = F_*/\alpha$. The equations

$$\begin{aligned}
\frac{\partial}{\partial t} b &= (m-1)\frac{F-1}{F+m-1} b \\
\frac{\partial}{\partial t} R_1 &= -m R_1 \int \frac{sb}{F+m-1} + \lambda'(\hat{R}_1 - R_1) \\
\frac{\partial}{\partial t} R_2 &= -m\alpha R_2 \int \frac{(1-s)b}{F+m-1} + \lambda'(\hat{R}_2 - R_2)
\end{aligned}$$

with $m = \mu/d$, $\lambda' = \lambda/d$, and $F = sR_1 + (1-s)R_2$. The condition for neutrality is

$$\langle \frac{F-1}{F-1+m} \rangle = 0 \quad or \quad 1 - \langle \frac{m}{F-1+m} \rangle = 0 \quad or \quad \langle \frac{1}{F-1+m} \rangle = \frac{1}{m}$$

If we use $\langle \frac{1}{x} \rangle \geq \frac{1}{\langle x \rangle}$,[†] we find that

$$\langle F \rangle \geq 1 \quad \text{or in dimensional terms} \quad \langle F \rangle \geq F_*$$

with equality holding only when $F$ is constant. Organisms faced with a fluctuating food supply require higher mean levels than the value which would suffice for a steady supply; this is true for all $s$ values. (Indeed this will hold in general for type II intake and mortality is independent of time.) If the needed increase in average food levels varies with $s$, we could expect exclusion of all the species except for the one with the minimum $\langle F \rangle$. If we look at the weakly fluctuating case $F = 1 + f'$, the growth rate is

$$\tilde{\sigma} \equiv \frac{\sigma}{m-1} = 1 - \langle \frac{1}{1 + f'/m} \rangle \simeq \frac{1}{m}\langle f' \rangle - \frac{1}{m^2}\langle f'^2 \rangle$$

with $f' = sR_1' + (1-s)R_2'$. The ESS will occur at some $\overline{s}$ where both $\sigma$ and $\frac{\partial \sigma}{\partial s}$ are zero. We find this point by taking $b = \overline{b}(t)\delta(s - \overline{s})$ and solving the time dependent equations to find the cycles of $\overline{R_1'}$ and $\overline{R_2'}$. We can then evaluate

$$\frac{\partial \tilde{\sigma}}{\partial s} = \frac{1}{m}\langle \frac{\partial f'}{\partial s} \rangle - \frac{2}{m^2}\langle f' \frac{\partial f'}{\partial s} \rangle$$

with $\frac{\partial f'}{\partial s} = \overline{R_1'} - \overline{R_2'}$. Since the second derivative of $f'$ is zero, we have

$$\frac{\partial^2 \tilde{\sigma}}{\partial s^2} = -\frac{2}{m^2}\langle \left( \frac{\partial f'}{\partial s} \right)^2 \rangle$$

[†] expand out

$$\left\langle \left[ \sqrt{\langle x \rangle / x} - \sqrt{x / \langle x \rangle} \right]^2 \right\rangle \geq 0$$

The second derivative is negative, so that we indeed expect to find a singular solution at the $\overline{s}$ point. Figure 6.18 shows the development of an isolated peak with seasonal forcing of $\hat{R}_1$ and $\hat{R}_2$; the exclusion times are long, depending on $\langle(\overline{R_1'} - \overline{R_2'})^2\rangle$. Note one special case: for a particular type of forcing, $R_1' = R_2'$ and $b = b_0(t)B(s)$ giving again a continuum solution. This requires $\int sB \big/ \int B = \alpha/(1+\alpha)$ and $\hat{R}_1 = \hat{R}_2$. In dimensional form, the latter condition just implies $\alpha\hat{R}_2 = \hat{R}_1$ – the time-variable resource supplies are always in the ratio required by the organisms' preference or nutritional value.

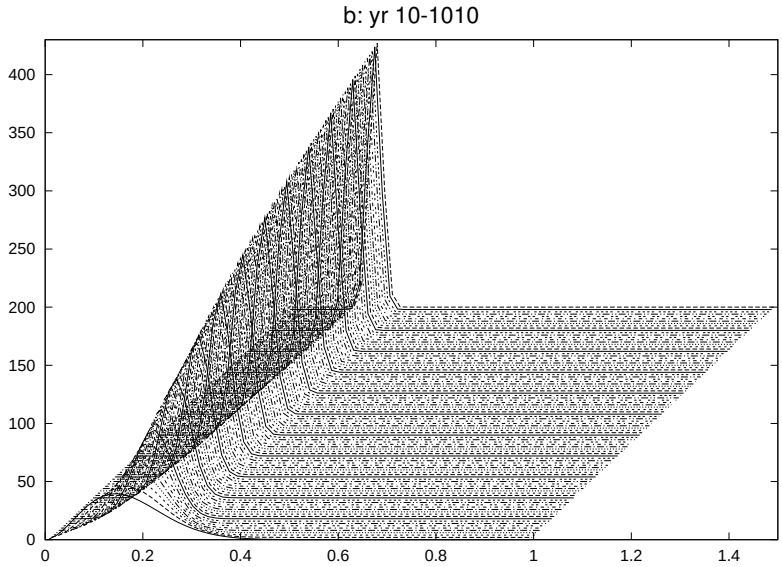


Figure 6.18: Year-to-year changes, tending to a singular solution in the periodically forced case. Snapshots do not show the yearly cycle, since only one was taken each year.

The latter suggests that perhaps $\alpha$ could also evolve. Assuming it is a decreasing function of $s$ – i.e., that organisms which prefer $R_2$ also gain more from using it than those which prefer $R_1$ – seems to lead to a split in the population with peaks at $s = 0$ and $s = 1$. The organisms which can use both are excluded.

### Two-d trait space

For trait spaces with higher dimensionality, locating the global (or local) ESS requires solving coupled nonlinear equations (when looking for the vanishing gadient of $\mathcal{R}$ in $\mathbf{s}$ space) or maximizing a complicated function of several or many variables. If they just interact to modify the uptake of a single resource, we may just have to maximize a function like $(\mu - d)/dN_h$ but with respect to multiple trait variables. For example, suppose we take our predator model and assign fractions of the animal to $s_0$ devoted to necessary functions (assumed constant), $s_1$ gut volume as before, and $s_2$ defense mechanisms. The rates of biomass increase by growth and reproduction are proportional to $1 - s_0 - s_1 - s_2$, $G_{max} \propto s_1$, and $\lambda \propto s_1^{2/3}$ as before. The death rate will be taken to be proportional to

$\exp(-\alpha s_2)$, reflecting increasing efficacity but never perfect defense. As in the nutrient uptake example eqn. 6.14, the ESS will maximize

$$\mathcal{R}_c = \frac{\lambda G_{max} - d}{\lambda d/\gamma}$$

(i.e., $\mu = \lambda G$, $N_h = \lambda/\gamma$ from 6.9) shown in $s_1$, $s_2$ space in fig. 6.19.

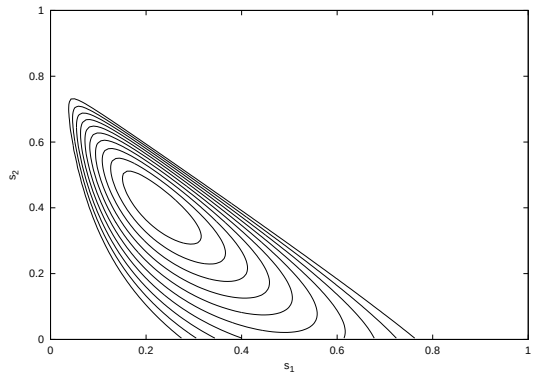


Figure 6.19: $\mathcal{R}_c d_0/\gamma_0 G_0$ for $d_0/\lambda_0 G_0 = 0.1$ and $\alpha = 5$.

While this figure shows the optimal state when the resources can be dpleted to a steady value, it is not sufficient when they or the parameters are varying in time. We can gain some insight for a system like

$$\mathcal{R} = \mu\ell(t)\frac{N}{N+N_h} - d = \mu\ell(t) - \mu N_h \frac{\ell(t)}{N+N_h} - d \quad ,$$

where both the uptake and nutrient level will be time-dependent, by regarding the steady nutrient level $R_* = N_h d/(\mu - d)$ and $u = \mu/d$ as the coordinates (figure 6.20). The transformation of coordinates is not one-to-one, as can be seen by the crossing lines, each of which has constant $s_2$.

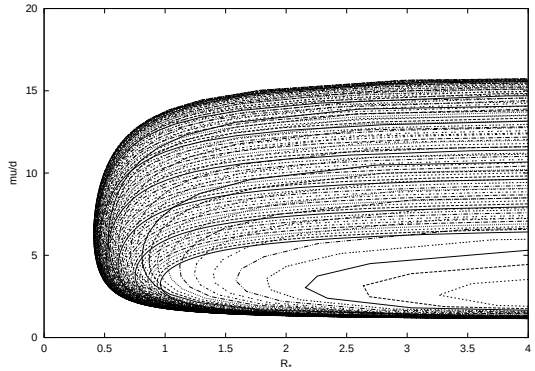


Figure 6.20: $R_*$, $\mu/d$ curves.

If we use $N_h = (u-1)R_*$, we can rewrite the net growth rate

$$\frac{1}{d}\mathcal{R} = \frac{u(\ell-1)N + (u-1)(N-R_*)}{N - R_* + ur_*} = u(\ell-1) + (u-1)\left[1 - \frac{u\ell R_*}{N - R_* + uR_*}\right]$$

The time-averaged growth rate is

$$G \equiv \langle \frac{1}{d}\mathcal{R} \rangle = u\langle \ell \rangle - 1 - (u-1)uR_* \langle \frac{\ell}{N - R_* + uR_*} \rangle \tag{6.18}$$

Suppose we start with a singular solution at a particular $\overline{s}$ value and integrate to a periodic (or, depending on the nature of the variability, statistically steady) state. If the resource reacts to the $b$, then we also find the cycle of $N$. Now we can find a line in $(R_*, u)$ space for which infinitesmal populations will neither grow nor decay. To see this, define

$$N_h = (u-1)R_*$$

(the half-saturation constant); the neutral line satisfies

$$u\left[\langle \ell \rangle - N_h \langle \frac{\ell}{N + N_h} \rangle\right] = 1$$

Given $N_h$ and knowing $\ell(t)$, $N(t)$, we can average in time to find $u$ and then set $R_* = N_h/(u-1)$. By using a range of $N_h$ values, we map out the neutral line. Organisms with traits such that they fall to the left of this line will be able to utilize lower resource values and will grow, This shows clearly in the simple steady case $\ell = 1$, $N = \text{const}$ when the growth rate is

$$G = (u-1)\frac{N - R_*}{N - R_* + uR_*}$$

which is zero for a constant value of $R_* = N$. Thus the neutral line exending from the chosen type is vertical, and organisms with a lower $R_*$ value will grow and exclude the original type. Therefore the types in the interior of the nose in figure 6.20 will be excluded. The surviving type will be the one for which the neutral curve is tangent to the boundary of the allowed region. For the steady case, with vertical neutral curves, this is the same as the type with the lowest $R_*$ value. But when the resource is varying, the neotral lines curve down and off to the left, so that the tangent point occurs at larger $u$ and $R_*$; figure 6.21 shows an example of this when the resource satisfies

$$\frac{\partial}{\partial t}N = -\int b\mathcal{R} + \lambda(N\hat{N}(t) - N)$$

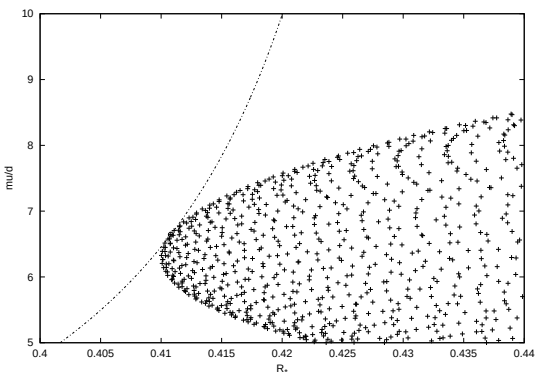

Figure 6.21: close-up of the possible states in $R_*$, $u$ coordinates, and the neutral curve from a particular $\mathbf{s}$ value. The points arise from a discretization in $\mathbf{s}$ space. $\hat{N}$ varies from 1 to 9 sinusoidally with a period of one year, while $\lambda = 1/100d$.

For this example, the changes are not dramatic, but the example illustrates the point that the ESS depends on the temporal characeristics of the environment, not just the mean. If the variations in $N$ and $\ell$ are weak, we can expand the $G = 0$ condition using 6.18 to find

$$R_* = \langle N \rangle - \frac{\langle N'^2 \rangle}{\langle N \rangle u} + \langle \ell' N' \rangle \quad , \quad \ell' = \ell - 1 \quad , \quad N' = N - \langle N \rangle$$

so that the neutral curves will indeed look like the one in figure 6.21.

As a second example, suppose the organism can allocate effort to acquiring nutrient $N_1$ or nutrient $N_2$ or to growth so that $V_j \propto s_j$ and $\mu_\infty \propto (1-s_1-s_2)$. If $Q_1/Q_{m,1} < Q_2/Q_{m,2}$, the expression which will be maximized (from 6.18) is

$$R = \frac{1}{N_{h,1}} \left[ \frac{\tilde{\mu}_\infty}{d} s_1 \tilde{v}_1 - \frac{s_1 \tilde{v}_1}{1 - s_1 - s_2} - 1 \right]$$

which will increase as $s_2$ and correspondingly $Q_2/Q_{m,2}$ decreases. Therefore the ESS should have colimitation with $Q_1/Q_{m,1} = Q_2/Q_{m,2}$. Secondly, we can maximize $R$ at a given $s_2$ to show that the ESS must lie on a curve

$$s_1 = 1 - s_2 - \sqrt{\frac{d}{\tilde{\mu}_\infty}(1 - s_2)}$$

As before, colimitation leads to 6.xx; therefore, we can scan along the line above, solving for $N_1 = Hd/(U - H)$, then using

$$\frac{Q_1/Q_{m,1}}{Q_2/Q_{m,2}} = \frac{s_1 \tilde{v}_1}{s_2 \tilde{v}_2} \frac{N_1}{N_1 + N_{h,1}} \frac{N_2 + N_{h,2}}{N_2} = 1 \tag{6.19}$$

to find $N_2$. We can then search for the value of $s_2$ such that 6.xx is satisfied. Figure 6.22 shows the line relating $s_1$ and $s_2$, the line from 6.xx with the appropriate $N_1$ value, and the distribution of $n(\mathbf{s})$ arrived at after xx years (beginning with a uniform distribution). The centroid of the population numbers has not reached the ESS point and th progress towards that has slowed significantly; the approach to the ESS takes long enough that we can doubt if it will reach that point before other environmental conditions change.

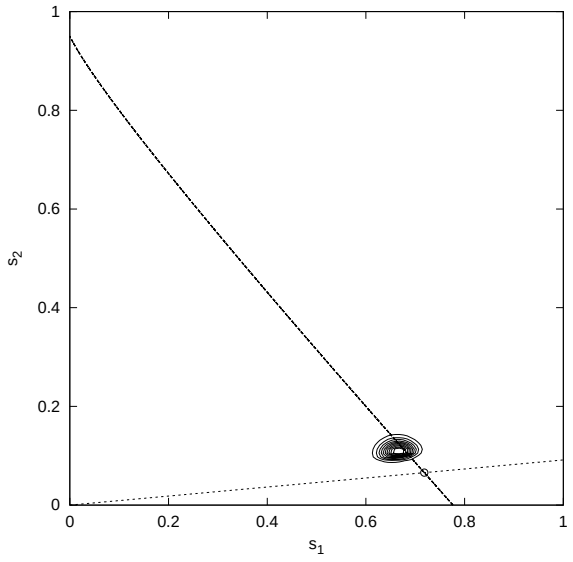


Figure 6.22: contours of $n$ superimposed on the lines relating $s_1$ and $s_2$; the small circle marks the ESS point. The value of $N_2/Q_{m,2} - N_1/Q_{m,1}$ is about $\frac{1}{2}$ the predicted value from 6,xx, yet is changing by only 2 parts per thousand in 10 years.

## 6.4 — Adaptive dynamics

Dieckmann and Law (19xx) point out that the dynamics may be approximated by equations for the net population and the rate of movement in trait space. As a simple, but analytically tractable example, consider a system with

$$\mathcal{R} = \left[R_0 - \frac{1}{2}R_2(s - s_0)^2\right]\left[1 - \frac{\langle b\rangle}{b_c}\right] - d$$

where $R_0$, $R_2$, $b_c$, $d$, and $s_0$ could be functions of time as the population or other processes alter the resource. We can find a time-dependent solution

$$b = b_0(t)\exp\left[-\frac{1}{2}\frac{[s - \overline{s}(t)]^2}{\sigma^2(t)}\right]$$

when

$$\begin{aligned}
\frac{\partial}{\partial t}\sigma^2 &= -R_2^*\sigma^4 + 2m \\
\frac{\partial}{\partial t}\overline{s} &= -R_2^*\sigma^2(\overline{s} - s_0) \\
\frac{1}{b_0}\frac{\partial}{\partial t}b_0 &= R_0^* - \frac{1}{2}R_2^*(\overline{s} - s_0)^2 - \frac{m}{\sigma^2} - d
\end{aligned}$$

with $R_j^* = R_j(1 - \sigma\sqrt{2\pi}\, b_0/b_c)$. The center of the distribution moves towards the peak in the growth rate curve at a speed which depends of the slope at the current center location

$[-R_2^*(\overline{s}-s_0)]$ and the square of the width of the distribution. The width asymptotes to the value $(2m/R_2^*)^{1/4}$ which narrows as the growth rate curve becomes more sharply peaked. The population will increase or decrease depending on the sign of of $R_0^* - m/\sigma^2 - d$; the dynamics of the resource will adjust $R_0^*$ until it reaches the equilibrium value.

The dominant species trait $\overline{s}$ will move up the gradient at a speed proportional to the gradient in $\mathcal{R}$ and to the covariance. The covariance increases because of mutation, but, if $\frac{\partial^2 \mathcal{R}}{\partial s^2}$ is negative, it will settle to a finite width.

For the more general problem, we define the net population biomass

$$\overline{b} = \int d\mathbf{r}\; b$$

the mean $r$ value

$$\overline{\mathbf{r}}\,\overline{b} = \int d\mathbf{r}\; b\,\mathbf{r}$$

and the variance

$$\sigma_{ij}\overline{b} = \int d\mathbf{r}\; b\; (r_i - \overline{r}_i)(r_j - \overline{r}_j)$$

These evolve according to

$$\begin{aligned}
\frac{\partial}{\partial t}\overline{b} &= \int d\mathbf{r}\; b\,\mathcal{R} \\
\frac{\partial}{\partial t}\overline{r}_i &= \overline{b}^{-1} \int d\mathbf{r}\; (r_i - \overline{r}_i) b\mathcal{R} \\
\frac{\partial}{\partial t}\sigma_{ij} &= \overline{b}^{-1} \int d\mathbf{r}\; \big[(r_i - \overline{r}_i)(r_j - \overline{r}_j) - \sigma_{ij}\big] b\mathcal{R} + 2m_i\delta_{ij}
\end{aligned}$$

If the distribution $b(\mathbf{r})$ is narrow, we can, at any given time, expand $\mathcal{R}$ around the current mean

$$\mathcal{R} \simeq \mathcal{R}(\overline{r}) + (r_i - \overline{r}_i)\frac{\partial \mathcal{R}}{\partial r_i} + \frac{1}{2}(r_i - \overline{r}_i)(r_j - \overline{r}_j)\frac{\partial^2 \mathcal{R}}{\partial r_i \partial r_j} = \mathcal{R}_0 + \mathcal{R}'_i(r_i - \overline{r}_i) + \frac{1}{2}\mathcal{R}''_{ij}(r_i - \overline{r}_i)(r_j - \overline{r}_j)$$

giving approximate equations

$$\begin{aligned}
\frac{\partial}{\partial t}\overline{b} &= \left[\mathcal{R}_0 + \frac{1}{2}\mathcal{R}''_{ij}\sigma_{ij}\right]\overline{b} \\
\frac{\partial}{\partial t}\overline{r}_i &= \sigma_{ij}\mathcal{R}'_j + \frac{1}{2\overline{b}}\mathcal{R}''_{jk}\int (r_i - \overline{r}_i)(r_j - \overline{r}_j)(r_k - \overline{r}_k) b \\
\frac{\partial}{\partial t}\sigma_{ij} &= \mathcal{R}'_k \overline{b}^{-1} \int d\mathbf{r}\; \big[(r_i - \overline{r}_i)(r_j - \overline{r}_j)(r_k - \overline{r}_k)\big] b \\
&\quad + \frac{1}{2}\mathcal{R}''_{km}\overline{b}^{-1} \int d\mathbf{r}\; \big[(r_i - \overline{r}_i)(r_j - \overline{r}_j)(r_k - \overline{r}_k)(r_m - \overline{r}_m)\big] b - \sigma_{ij}\sigma_{km} + 2m_i\delta_{ij}
\end{aligned}$$

If we make the quasi-normal approximation, assuming that $b$ is close to a Gaussian function, these simplify to

$$\begin{aligned}
\frac{\partial}{\partial t}\overline{b} &= \left[\mathcal{R}_0 + \frac{1}{2}\mathcal{R}''_{ij}\sigma_{ij}\right]\overline{b} \\
\frac{\partial}{\partial t}\overline{r}_i &= \sigma_{ij}\mathcal{R}'_j \\
\frac{\partial}{\partial t}\sigma_{ij} &= \frac{1}{2}\mathcal{R}''_{km}\left[\sigma_{ik}\sigma_{jm} + \sigma_{im}\sigma_{jk}\right] + 2m_i\delta_{ij} \\
&= \sigma_{ik}\mathcal{R}''_{km}\sigma_{mj} + 2m_i\delta_{ij}
\end{aligned} \tag{6.20}$$

(using the fact that both $\mathcal{R}''_{km}$ and $\sigma_{ij}$ are symmetric). The dominant species traits $\overline{\mathbf{r}}$ will move up the gradient (even though $\mathcal{R}(\overline{r}) = 0$) at a speed proportional to the gradient in $\mathcal{R}$ and the covariance. The covariance increases because of mutation, but, if $\mathcal{R}''_{km}$ is negative, it will settle to a finite width as in the simplified case.

The environment will be time-dependent because of many external factors, so that $\mathcal{R}$ itself has a whole spectrum of variability. The velocity for movement in trait space will therefore be fluctuating, and we cannot expect the system to be in equilibrium. If the external changes are very slow compared to mutation times, the system will be very close to the ESS for current conditions:

$$\frac{\partial\mathcal{R}(\mathbf{s},t)}{\partial s_i}\Big|_{\mathbf{s}=\overline{\mathbf{s}}(t)} \simeq 0$$

In contrast, if the environmental fluctuations are fast, the center of the distribution will not be able to keep up, and the mean trait value will settle at the point where the time-averaged velocity is zero

$$\left\langle \frac{\partial\mathcal{R}(\mathbf{s},t)}{\partial s_i}\Big|_{\mathbf{s}=\overline{\mathbf{s}}} \right\rangle \simeq 0$$

For intermediate time-scales, comparable to mutation times, the center of the distribution will partially, but not completely, track the variations. The population dynamics is implicit here, basically maintaining $\mathcal{R}(\overline{s},t)$; as we shall see, it may play a much more active role with multiple trophic levels.

When w have local competition as in Fig. 6.6 or, as we shall see, loalized predation, we need to define a localized form of adaptive dynamics. We represent $b$ as a sum of near-delta functions

$$b = \overline{b}_i(t)\phi(\mathbf{s} - \mathbf{s}_i)$$

where $\phi$ is symmetric, has integral 1, and is localized in a small region around argmuent 0. Keeping only the first terms in the Taylor expansion or $\mathcal{R}$ gives

$$\begin{aligned}
\frac{\partial}{\partial t}\overline{b}_i &= \mathcal{R}(\mathbf{s}_i, N)\overline{b}_i \\
\frac{\partial}{\partial t}\mathbf{s}_{i,j} &= \sigma\frac{\partial\mathcal{R}}{\partial s_j}\Big|_{\mathbf{s}=\mathbf{s}_i}
\end{aligned} \tag{6.21}$$

The functionals of $b$ implicit in $N$ will turn into functions of the $b_i$'s. If we are concerned with finding steady end states, the value of $\sigma$ will affect the approach time, but not the final values. These equations can be stepped forward; when two "species" get too close, they can be merged into one. As an example, we show the case considered in Fig. 6.6, showing that indeed the stable final state has biota with six distinct traits; if we start with fewer, the final equilibrium shows that neighboring types can grow, whereas starting with more leads to mergers until the six remain.

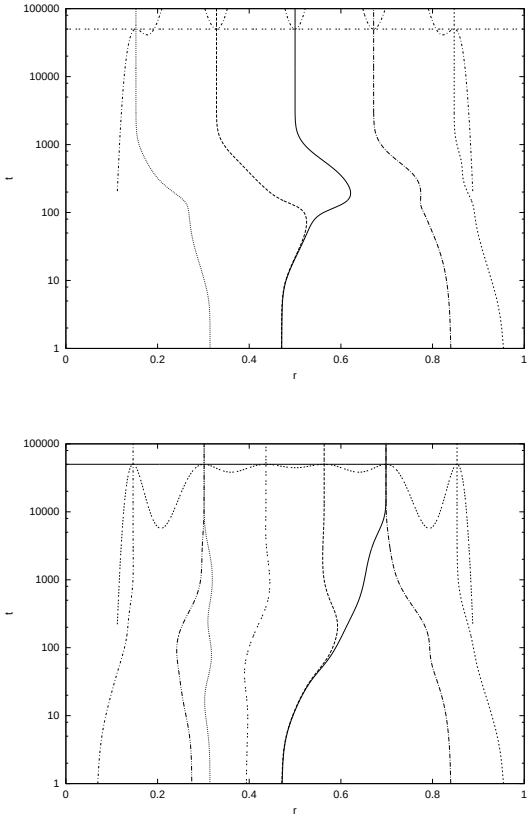


Figure 6.23: Adaptive dynamics solutions for the $r$ values in 6.6 plotted against $\log(t)$. The upper panel starts with 5 types and the lower with 8. The growth rate vs. continuous $r$ at the end of the integratio is shown with the vertical line being the zero value and positive values to the right. The case with 8 types settles to an ESS with 6 distinct points.

These solutions show that a steady state for the lowest order adaptive dynamics solution with $N$ types may nevertheless be unstable to the introduction of biomass with a different trait.

## 6.5 — Predation/ food webs

We now consider predation, which transfers biomass from one region to another in an enlarged trait space which, for organisms with trait $\mathbf{s}$, includes information about their prey and their predators. For simplicity, we begin with a generalization of the QNPZ model; the biotic part can be written

$$\mathcal{R} = L(\mathbf{s}) + \int ds'\, M(\mathbf{s}, \mathbf{s}') b(\mathbf{s}') \tag{6.22}$$

where the linear term $L$ includes uptake of abiotic resources ($N$) and death rates while the nonlinear terms represent the rate at which organism $\mathbf{s}$ grazes upon $\mathbf{s}'$, $M(\mathbf{s}, \mathbf{s}') > 0$, or $\mathbf{s}$ is eaten by $\mathbf{s}'$, $M(\mathbf{s}, \mathbf{s}') < 0$. The trait variable $\mathbf{s}$ here can be partitioned into a set of values corresponding to autotrophs ($L(\mathbf{s}) > 0$, $M(\mathbf{s}, \mathbf{s}') \leq 0$) and heterotrophs ($L < 0$ and $M(\mathbf{s}, \mathbf{s}') > 0$ for some prey $\mathbf{s}'$). In terms of a discretized version, the pure QNPZ matrices would have a block structure like

$$L \sim \begin{pmatrix} + \\ - \end{pmatrix} \quad , \quad M \sim \begin{pmatrix} 0 & - \\ + & 0 \end{pmatrix} \quad \text{for} \quad \begin{pmatrix} P \\ Z \end{pmatrix}$$

But this more general structure also permits mixotrophs which can have both $L$ and $M$ positive. We also note that intra-species competition can enter as $M(\mathbf{s}, \mathbf{s}') < 0$ for $\mathbf{s}'$ in a small enough neighborhood of $\mathbf{s}$ so that the organisms resemble each other clearly enough to compete.

Our autotroph example 6.3 has

$$L = g_m(s) - d(s) \quad \text{and} \quad M(s, s') = -g_m(s)/b_c(s)$$

(independent of $s'$ so that the integral just yields $-g_m \langle b \rangle / b_c$). Now, however, we turn to the QNPZ system. We partition $s_{orig}$ into two segments $r = r_0 s_{orig}$ for $0 \leq s_{orig} < 0.5$, representing the phytoplankton and $s = s_0(s_{orig} - 0.5)$ for $0.5 \leq s_{orig} < 1$ for the zooplankton. With $N = N_T - \int dr P - \int ds Z$, the linear and nonlinear terms become

$$L = \begin{pmatrix} \mu(r) N_T - d_p(r) \\ -d_z(s) \end{pmatrix} \quad \text{and} \quad M = \begin{pmatrix} -\mu(r) & -\mu(r) - G(s', r) \\ a(s) G(s, r') & 0 \end{pmatrix}$$

with the integrations occuring over the primed variables and $G(s, r)$ giving the rate of $Z(s)$ grazing on $P(r)$. Writing these out less compactly makes the similarity to Moloney and Fields (19xx) discrete model obvious:

$$\begin{aligned} \frac{\partial}{\partial t} P(r) &= \left[ \mu(r) N - \int ds\, Z(s) G(s, r) - d_P(r) \right] P(r) \\ \frac{\partial}{\partial t} Z(s) &= \left[ a(s) \int dr\, G(s, r) P(r) - d_Z(s) \right] Z(s) \end{aligned} \tag{6.23}$$

Both forms are useful; we shall work with the explicit one for simplicity, but comment upon the somewhat more general one 6.22 when possible. To simplify the derivations further,

we shall partition $G(s,r)$ into a part giving the maximum rate for ZP with trait $s$ and a part depending on the ratio of the prey and predator weights. If we take the traits to be log weight [or more precisely $r = \ln(w/w_{0p})$, $s = \ln(w/w_{0z})$], then

$$G(s,r) = g_m(s)\Phi(s-r)$$

with $\Phi \leq 1$. By choosing the $w_0$ factors appropriately, we can move the maximum to $r = s$; if the preferred prey's weight is $\frac{1}{10}$ of the predator's, then we just choose $w_{0s} = 10w_{0r}$.

We comment that food limitation can be included by making $G$ into a functional of $b$; for example,

$$G(\mathbf{s},\mathbf{s}',b) = \frac{g_m(\mathbf{s})\Phi(\mathbf{s},\mathbf{s}')}{P_h(\mathbf{s}) + \int d\mathbf{s}''\,\Phi(\mathbf{s},\mathbf{s}'')b(\mathbf{s}'')}$$

(remembering that $G$ represents grazing by type $\mathbf{s}$ on $\mathbf{s}'$). Most of the approaches used below in the quadratic case carry through in the M-function case, though results may differ.

### 6.5.1 — Singular solutions

As usual, we can find singular solutions to 6.23 using

$$P = \overline{P}(t)\delta(r-\overline{r}) \quad , \quad Z = \overline{Z}(t)\delta(s-\overline{s})$$

and recovering the equation xx.xx with the interaction coefficient being $G(\overline{s},\overline{r})$. Now, however, we focus on determining when this state is an ESS by postulating

$$P = \overline{P}(t)\delta(r-\overline{r}) + P'(t)\delta(r-r') \quad , \quad Z = \overline{Z}(t)\delta(s-\overline{s}) + Z'(t)\delta(s-s')$$

The steady state for the ZP equation

$$a(\overline{s})g_0(\overline{s})\Phi(\overline{s}-\overline{r})\overline{P} = d_Z(\overline{s})$$

can be combined with the equation for the growth rate at $s'$

$$\frac{1}{Z'}\frac{\partial}{\partial t}Z' = a(s')g_0(s')\Phi(s'-\overline{r})\overline{P} - d_z(s')$$

leading to the condition that $\overline{s}$ be the ESS

$$\frac{a(s')g_0(s')\Phi(s'-\overline{r})}{d_z(s')} < \frac{a(\overline{s})g_0(\overline{s})\Phi(\overline{s}-\overline{r})}{d_z(\overline{s})}$$

We assume that $a(s)g_0(s) = d_Z(s)P_0$ with $P_0$ constant; in the case of traits being log weight, this gives equilibria with equal PP biomass in each log weight class (as in xx.xx). For the singular solution, $\overline{P} = P_0$. The condition above becomes

$$\Phi(s'-\overline{r}) < \Phi(\overline{s}-\overline{r})$$

We have the freedom in choosing the base weights so that we can make $\Phi(x)$ to have be maximal at $x = 0$ with a value of 1 (therebye setting $g_0(s)$). For the ZP, then, $\overline{s} = \overline{r}$ represents the ESS.

For the PP, the situation is less simple. The criterion

$$\mu(r')\overline{N} - g_0(\overline{s})\Phi(\overline{s} - r')\overline{Z} - d_p(r') < \mu(\overline{r})\overline{N} - g_0(\overline{s})\overline{Z} - d_p(\overline{r})$$

The local extremum condition is

$$\mu'(\overline{r})\overline{N} - d'_P(\overline{r}) = 0$$

since $\Phi' = 0$ from the ZP equation. We shall take $d_P$ to be constant or even zero, in which case the extremum condition is just that $\mu$ obtains its maximum value at $\overline{r}$. The case with $d_P = 0$ (all PP death occuring from predation), gives a growth rate for PP with different traits

$$\mathcal{R}_P = \mu(\overline{r})\overline{N}\left[\frac{\mu(r')}{\mu(\overline{r})} - \Phi(\overline{s} - r')\right]$$

Both $\mu(r')$ and $\Phi(\overline{s} - r')$ are parabolic with maxima at $r' = \overline{r}$. The growth rate will be negative if

$$\frac{|\Phi''(0)|}{\Phi(0)} < \frac{|\mu''(\overline{r})|}{\mu(\overline{r})}$$

(both second derivatives being negative); the extremeum will be a local ESS if the PP growth rate is more sharply peaked than the grazing function.

We parameterized the traits $r$ and $s$ such that $\Phi(s - r$ has its maximum at zero; likewise, we can shift $r$ such that the maximum of $\mu$ is at $r = 0$.

$$\mathcal{R} \sim \mu_0(\overline{r})\overline{N} - d_P - g_0(\overline{s})\overline{Z} + \frac{1}{2}(g_0(\overline{s})\Phi_2\overline{Z} - \mu_2\overline{N})r^2$$

The first three terms cancel, so that the $r = s = 0$ point will be stable or unstable depending on whether $g_0(\overline{s})\overline{Z}\Phi_2$ is less than or greater than $\mu_2\overline{N}$. A narrow grazing kernel ($\Phi_2$ large) and a wide nutrient uptake function $\mu_2$ small) will tend to be unstable. The net growth rate for PP, in the absence of ZP, is parabolic, with the peak above zero. The grazing depresses this curve until the former peak rests at zero. When the grazing kernel is wide, the whole parabola moves down enough so that the $r = 0$ point is an ESS. However, when the grazing kernel is narrow, it only makes a dip in the net growth rate such the the $r = 0$ point goes to zero leaving the growth rate positive on either size (figure 6.24).

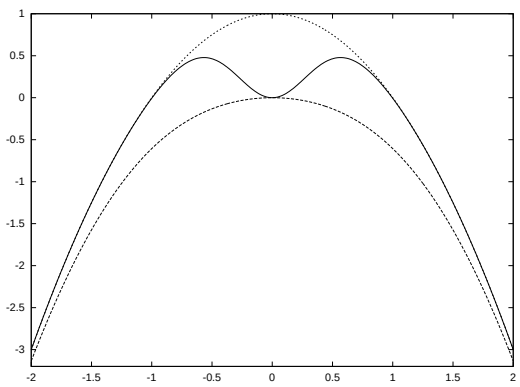

Figure 6.24: sketches of the net PP growth rate iwth a narrow Gaussian grazing kernel, a wide kernel (dahed), and no grazing (dotted).

When $d_P = 0$, the equilibrium has $\overline{Z} = \mu_0 \overline{N}/g_0$, and the growth rate becomes

$$\mathcal{R} \sim \frac{1}{2}\mu_0 \overline{N} \left( \Phi_2 - \frac{\mu_2}{\mu_0} \right) r'^2$$

The solution with $\overline{r} = \overline{s} = 0$ is no longer stable when $\Phi_2 > \mu_2/\mu_0$.

With the slightly more general case

$$b = b_i(t)\delta(s - \overline{s}_i)$$

(with the previous case having only two values for $i$), the steady state equations for $\overline{b}$ become

$$M(\overline{s}_i, \overline{s}_j)\overline{b}_j = -L(\overline{s}_i) \tag{6.24}$$

can be combined with the linearized equations for the perturbations at different $s'$ values

$$\begin{aligned} \frac{1}{b'_i}\frac{\partial}{\partial t} b'_i &= L(s'_i) + M(s'_i \overline{s}_j)\overline{b}_j \\ &= L(s'_i) - M(s'_i, \overline{s}_j) M(\overline{s}_k, \overline{s}_j)^{-1} L(\overline{s}_k) \end{aligned}$$

to determine the ESS condition:

$$L(s'_i) < M(s'_i, \overline{s}_j) M(\overline{s}_k, \overline{s}_j)^{-1} L(\overline{s}_k)$$

for $s'_i \neq \overline{s}_i$. These must hold simultaneously for all values of $i$. It will generally be easier to find the values of $\overline{s}_i$ by examining the condition for a local extremum

$$\frac{\partial L(s_i)}{\partial s_i} = \frac{\partial M(s_i, \overline{s}_j)}{\partial s_i} M(\overline{s}_k, \overline{s}_j)^{-1} L(\overline{s}_k) \tag{6.25}$$

with the derivatives evaluated at $s_i = \overline{s}_i$. Once found, we can test whether they are maxima or not.

### 6.5.2 — Bifurcations

Weitz, et al. (20xx) examined the adaptive dynamics approach to analyze the behavior when the $\overline{r} = \overline{s} = 0$ state is not an ESS. Like their equations, ours have the simplest quadratic nonlinearity, although we use a continuous traait space rather than stochastic mutation and sampling. In the siplest form, we have

$$\begin{aligned}
\frac{\partial}{\partial t}\overline{P} &= \left[\mu(\overline{r})N - \overline{Z}G(\overline{s},\overline{r}) - d_P(\overline{r})\right]\overline{P} \\
\frac{\partial}{\partial t}\overline{Z} &= \left[a(\overline{s})G(\overline{s},\overline{r})\overline{P} - d_Z(\overline{s})\right]\overline{Z} \\
\frac{\partial}{\partial t}\overline{r} &= \sigma_{PP}\left[\mu'(\overline{r})N - \overline{Z}\frac{\partial G(\overline{s},\overline{r})}{\partial \overline{r}} - d'_P(\overline{r})\right] \\
\frac{\partial}{\partial t}\overline{s} &= \sigma_{ZZ}\left[\frac{\partial [a(\overline{s})G(\overline{s},\overline{r})]}{\partial \overline{s}}\overline{P} - d'_Z(\overline{s})\right]
\end{aligned}$$

with $N = N_T - \overline{P} - \overline{Z}$. Near the origin (in the simplest case with $d_P = 0$ and $g_0$, $a$, $d_Z$ constant), the last two equations for the mean trait values become

$$\begin{aligned}
\frac{\partial}{\partial t}\overline{r} &= \sigma_{PP}\left[\mu''\overline{N}\,\overline{r} - g_0\Phi''\overline{Z}(\overline{r}-\overline{s})\right] \\
\frac{\partial}{\partial t}\overline{s} &= \sigma_{ZZ}\left[ag_0\overline{P}\Phi''(\overline{s}-\overline{r})\right]
\end{aligned}$$

The determinant is positive, so that instability requires

$$\sigma_{PP}\,\mu_0\overline{N}\left(\Phi_2 - \frac{\mu_2}{\mu_0}\right) > \sigma_{ZZ}d_Z\Phi_2$$

If $\sigma_{ZZ}/\sigma_{PP}$ is large enough, the origin is stable in the adaptive dynamics equations; otherwise, the mean traits develop a limit cycle (fig. 6.25) The adaptive dynamics picture seems clear: the PP mutate away from $r = 0$. If the ZP mutate slowly, the PP will find a new ESS at some finite $r$. But the ZP mutations will slowly decrease $|s - r|$ and the PP will begin shifting back until there is no local maximum and they move quickly to the other side of the origin. For the case sketched in fig 6,24, we can find the $\overline{r}(\overline{s})$ such that the $Z$ nd $N$ are in equilibrium and $\frac{\partial}{\partial t}\overline{r} = 0$. E.g., for

$$\mathcal{R}_P = \left(\mu_0 - \frac{1}{2}\mu_2\overline{r}^2\right)\overline{N} - g_0\exp\left(-\frac{1}{2}\Phi_2[\overline{s}-\overline{r}]^2\right)\overline{Z}$$

the equilibrium population balances the two terms, while the trait migrates according to

$$\begin{aligned}
\frac{\partial}{\partial t}\overline{r} = \frac{\partial \mathcal{R}_P}{\partial r} &= \sigma_{PP}\left(-\mu_2\overline{N}\overline{r} + \Phi_2[\overline{r}-\overline{s}]g_0\exp\left(-\frac{1}{2}\Phi_2[\overline{s}-\overline{r}]^2\right)\overline{Z}\right) \\
&= \sigma_{PP}\mu_0\overline{N}\left(-\frac{\mu_2}{\mu_0}\overline{r} + \Phi_2[\overline{r}-\overline{s}]\left[1 - \frac{1}{2}\frac{\mu_2}{\mu_0}\overline{r}^2\right]\right)
\end{aligned}$$

The vanishing of the term in parentheses gives the relation superimposed on fig. 6.25; the limit cycle is basically a relaxation oscillation around this hysteresis curve. When the ZP mutate more rapidly, they keep up with the PP, so that the $\frac{\partial}{\partial t}\overline{s}$ equation is inequilibrium and $\overline{s}$ is nearly equal to $\overline{r}$ at all times. The second term in $\frac{\partial}{\partial t}\overline{r}$ is negligible, and $\overline{r}$ is driven back to zero by the first term.

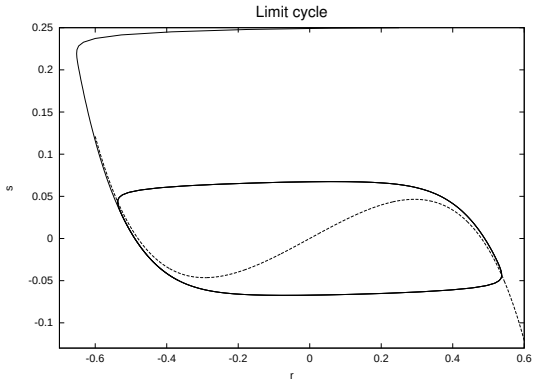


Figure 6.25: Limit cycle for $\sigma_{PP} = 25\sigma_{zz}$ with $\mu_2 = 2\mu_0$ and $\Phi_2 = 2.6$. The dashed line shows the realtionship between $\overline{r}$ and $\overline{s}$ in equilibrium.

Unfortunately, these scenarios do not agree with the full model even when mutation included. Fig. 6.26 shows that for both small and large ratios of the ZP mutation rate to that of the PP, the distributions settle to a steady state with two dominant $P$ "species" and one $Z$. The steady state is approached by dampled oscillations, as one or the other PP stypes dominates and the ZP distribution shifts towards the dominant side, leaving the other able to grow. Mutation enahnces this process, but does not permit continuing oscillations.

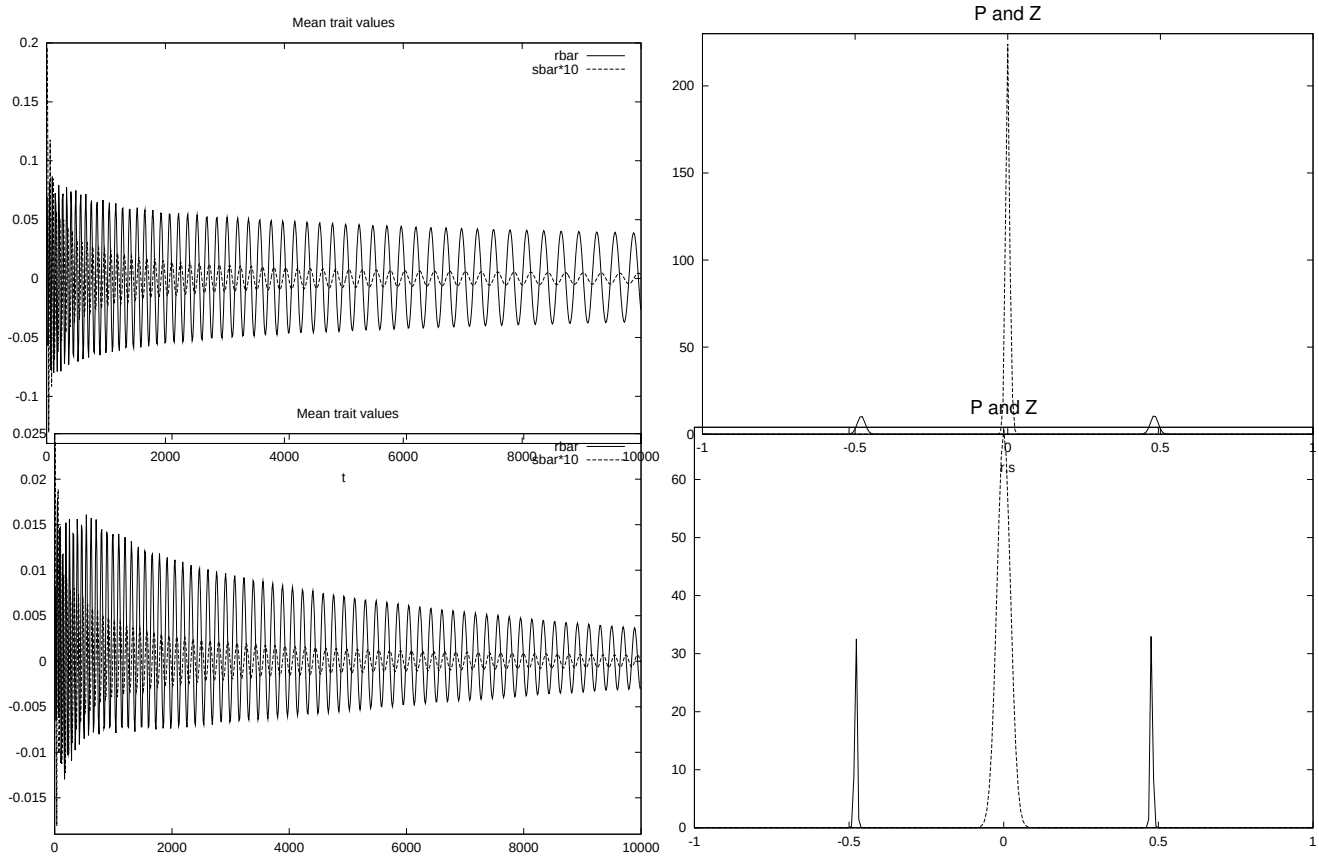


Figure 6.26: Two examples showing the decaying oscillations and the approach to a state with two $P$ types and one $Z$. The first has the mutation rate for PP 100 times larger than for $ZP$; the second has the opposite.

If we try an adaptive dynamics experiment with many initial types, merging them when they approach closely enough, and using $\sigma_{PP} = \sigma_{ZZ}$ for added stability, we reproduce the 2 $P$, 1 $Z$ final state with the growth rates showing all three points are local maxima in growth rates, and the combination is a global ESS (fig. 6.27). Adaptive dynamics can, indeed, give the proper answer, but starting from many types and sorting them out rather than letting a single one evolve.

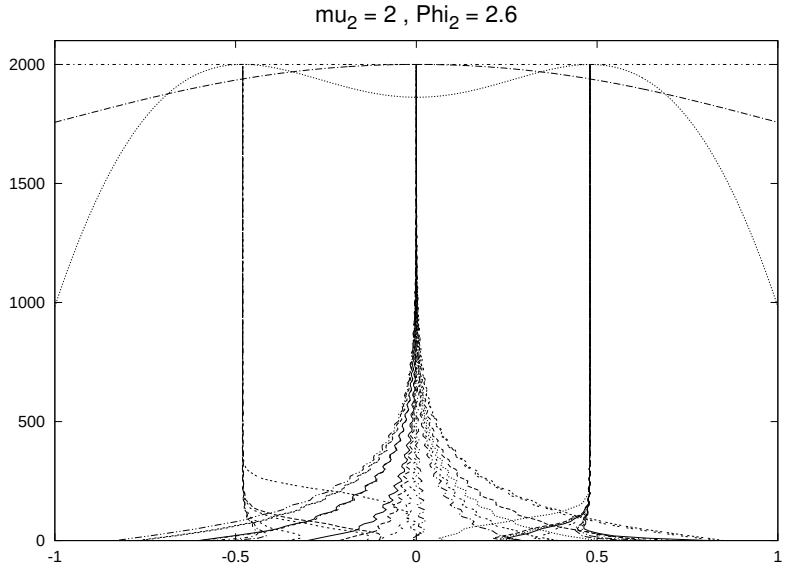


Figure 6.27: Movement in trait space starting with 15 initial prey and 15 predator types. The growth rates, $\mathcal{R}_P$ and $\mathcal{R}_Z$, are shown at the final time.

With this insight, we can look for solutions as $\Phi_2$ gets larger and larger, corresponding to narrower grazing kernels. We find a sequence of bifurcations labelled by the number of PP types and the number of ZP types: 1,1 $\rightarrow$ 2,1 $\rightarrow$ 2,2 $\rightarrow$ 3,2 $\rightarrow$ 3,3 etc. Odd numbers have a type reappearing at the original maxima $\overline{r} = \overline{s} = 0$. Apparently, these states are stable to invading species with other traits, as shown by the $\mathcal{R}_P$ and $\mathcal{R}_Z$ curves. In addition, the population dynamics shows that thes states are neutral, with some decaying eigenvalues and some oscillatory ones. In the 2,2 case, the nonlinear terms do lead to damping; however, the derivation is lengthy and difficult to do for higher $\Phi_2$ cases. The numerics, on the other hand, show that oscillations in the values of $\overline{P}$ and $\overline{Z}$ also damp out.

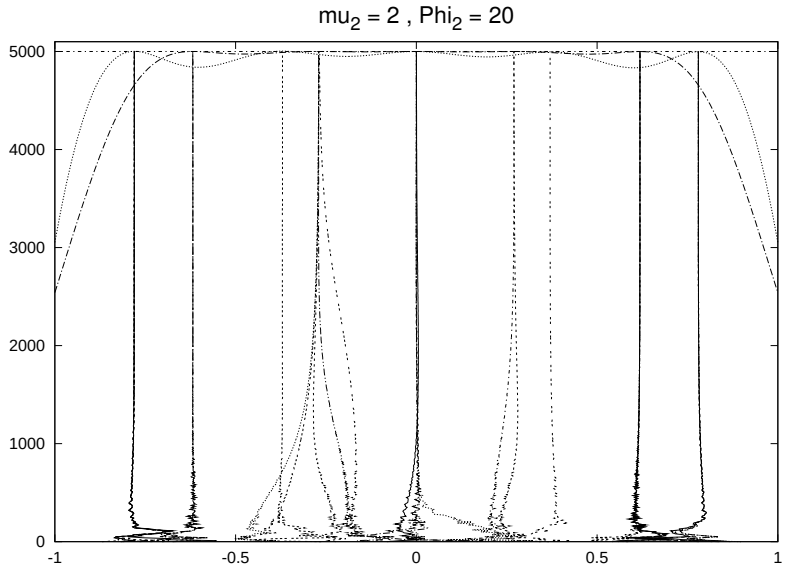

Figure 6.28: As in 6.27, but with a larger $\Phi_2$ value, sowing the evolution to a 5,5 system.

### 6.5.3 — Continuum solutions

The results in the previous section are quite different from those in Chapter xx, where we found smooth solutions to the coupled NPZ system. The difference lies in the form of the grazing kernel. The steady states are solutions to the Fredholm integral equations of the first kind

$$\int d\mathbf{s}' M(\mathbf{s}, \mathbf{s}') b(\mathbf{s}') = -L(\mathbf{s})$$

Given the form of the uptake and grazing functions, and thereby of $M$ and $L$, will there be non-negative solutions and will there be regular solutions?

If we continue with the grazing of the form $g_0(s)\Phi(s-r)$ and the same allometric scaling $d_z(s) = a(s)g_0(s)P_0$ with $P_0$ constant, we require

$$\int dr\, \Phi(s-r)P(r) = P_0$$

for a finite range of $s$ values. In Chapter xx, we looked at the same problem but as size-spectrum models; in the current context, if the traits are again weight or its log, we are asking whether particular weights would be favored.

As an example which can be solved analytically, we consider an exponential grazing kernel with a cutoff for $r > s$. When the traits are log weight, this means predators prefer prey smaller than some fixed fraction of their own weight, with the preference decreasing as some power of the weight ratio

$$\Phi(s-r) \propto e^{-\lambda(s-r)} (s \geq r)$$

where the PP and ZP weights are scaled so that $s = r$ corresponds to (for example) $w_P = \frac{1}{10} w_Z$. We can also choose the range of possible weights to correspond to trait values between 0 and 1. When discretized, the miximum prey to predator size ratio cutoff gives a lower trianglular matrix, ensuring the existence of solutions. We can also normalize

$$\Phi(s-r) = n(s)e^{-\lambda(s-r)}\ (s \geq r)$$

with $n$ chosen sothat the intergal of $\phi$ is one: $n = (1 - e^{-\lambda s})/\lambda$. But we'll retain the $n(s)$ notation for generality.

Using solutions to the integral equations

$$\begin{aligned}
&\int_a^s dr\ e^{-\lambda(s-r)} P(r) = f(s) \Rightarrow P(r) = f(a)\delta(r-a) + \lambda f(r) + \frac{d}{dr} f(r) \\
&\int_r^b ds\ e^{-\lambda(s-r)} \tilde{Z}(s) = f(r) \Rightarrow \tilde{Z}(s) = \frac{Z(s) g_m(s)}{n(s)} = f(b)\delta(s-b) + \lambda f(s) - \frac{d}{ds} f(s)
\end{aligned} \tag{6.26}$$

The continuum solutions are

$$P = P_0(r_0)n(r_0)\delta(r - r_0) + \lambda P_0(r)n(r) + \frac{d}{dr}[P_0(r)n(r)] \tag{6.27}$$

where $P_0(r) = d_z(r)/g_0(r)a(r)$ and

$$Z(s) = \frac{n(s)}{g_0(s)}\left[Z_0(s_1)\delta(s - s_1) + \lambda Z_0(s) - \frac{d}{ds}Z_0(s)\right] \tag{6.28}$$

with $Z_0(s) = \mu(s)N - d_p(s)$. We choose the smallest value of $r_0$ (the minimum PP weight) and the largest value of $s_1$ (the maximum ZP weight) such that both of these are everywhere positive. We can then iterate on the choice of $N$ until $N + \int dr\, P(r) + \int ds\, Z(s) = N_T$.

In the case of pure allometric scalings with $\exp(-\beta' s)$ forms, $P_0$ constant, and a normalized grazing kernel, the maximum wieght has $\mu(s_1)N = d_p(s_1)$ while the minimum weight is zero with $n(0) = 0$. As a result, the amplitudes of the singular solutions are zero. Now $P = P_0$ and

$$Z = \frac{1 - e^{-\lambda s}}{\lambda g_0 e^{-\beta' s}}\left[(\lambda + \beta')\mu_0 N e^{-\beta' s} - \lambda d_p\right]$$

and we can find the relationship between $N$ and $N_T$ explicitly. However, adding the constraint $\mu(s_1)N = d_p$ leads to a transcendental equation for $N$; this can be iterated to a solution rapidly.

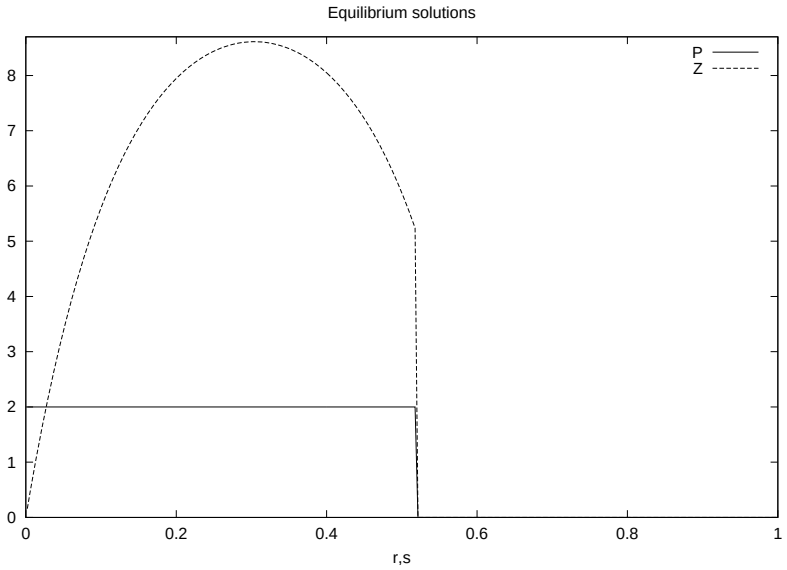


Figure 6.29: Example of stable continuum solutions with $\lambda = \beta' = 8$, $\mu_0 = 1.5$, $g_0 = 0.125$, $a = 0.6$, $d_P = 0.01$, $d_{Z0} = 0.15$, ($P_0 = 2$), and $N_T = 5$.

The sudden drop of $Z$ to zero for $s > s_1$, although clear from 6.28, seems odd, since the ZP for $s$ slightly larger than $s_1$ still have a food supply very similar to that for $s$ slightly smaller. But they are being out-competed: their growth rate is somewhat smaller because of the $g_0(s)$ factor and the fact that $\Phi$ is a little further down the exponential tail.

A similar disadvantage appears ass $s \to s_1$, but it is offset by a new food supply at $r = s$ which the smaller ZP cannot tap. This no longer exists for $r, s > s_1$ since $\mu(r)N < d_p$ and the PP cannot survive. Thus, some form of competitive exclusion persists even in these continuous solutions.

### 6.5.4 — Mixed solutions

The general solutions above suggest we should also see mixed cases with singularities and also smooth parts. As an example, suppose that $\mu$ drops back to zero as $s \to 0$. Then $Z_0$ will be negative and $\frac{d}{ds}Z_0$ will be positive for small $s$ values, so that 6.28 will give negative values for $Z(s)$. Since the $Z$ solution comes from the PP equation, the negative values indicate the combination of low $\mu$ and grazing pressure from the positive ZP at higher $S$ values prevents growth of the autotrophs. Therefore, $r_0$ will be greater than zero, $n(r_0)$ will be positive, and the singular contribution in 6.27 will be non-zero.

To solve, we begin with an estimate of $N$. That gives us the value of $s_1$ where $Z_0 = 0$ and $r_0$ where $\lambda Z_0 = d/ds Z_0$. $P$ has the singularity as $r_1$ and the continuum solution in the range $r_0 < r < s_1$ (6.27) and $Z$ satisfies 6.28. We can then compute total $N + \int P + \int Z$ and adjust $N$ until this matches $N_T$; an example is shown in figure 6.30.

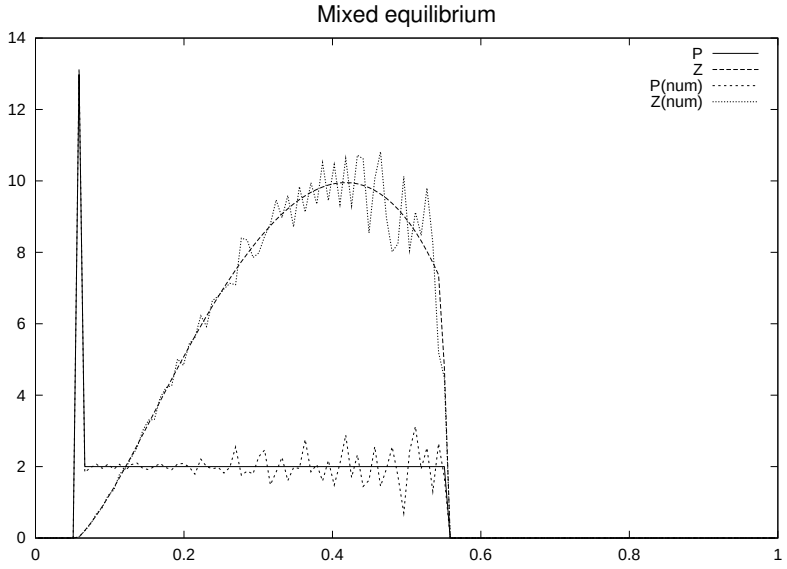


Figure 6.30: Mixed solution superimposed on the numerical solution after 1000 years. $\Delta r = 1/128$. The growth rate is $6r(1-r)e^{-8r}$. The singularity is integrated over $\Delta r$ in both curves.

If we do not normalize the grazing kernel, then 6.28 likewise has a singular contribution, now in the smallest possible size, and a continuum distribution extending up to the point where $Z_0$ vanishes. The ZP maximum occurs in the smallest size class, with $Z$ decaying weakly for larger $s$.

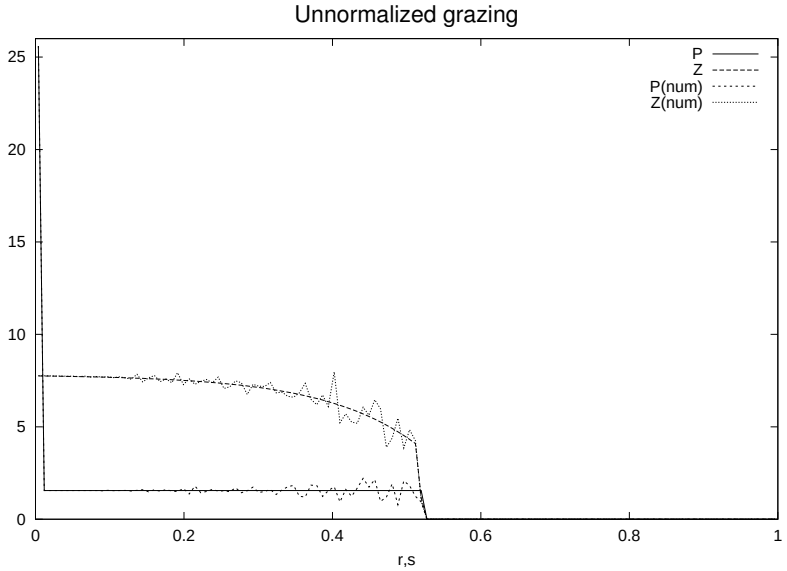


Figure 6.31: As in 6.29 but for $n(s) = 1$ and $g_0 = 1.25$.

### 6.5.5 — Peaked uptake and grazing kernels

We might expect that the grazing kernel is peaked with a smoot transition to 0.; e.g.,

$$\Phi(s-r) = n(s)(s-r)e^{-\lambda(s-r)}(s \geq r) \tag{6.29}$$

If we normalize in the same way, the equation for $P9R$) is just $-\frac{\partial}{\partial\lambda}$ of the first equation in 6.26; therefore, the solutions remain the same. However, the $Z$ equation does change, developing a singularity at the large $s$ end:

$$\tilde{Z}(s) = \left[\frac{\partial^2 f}{\partial s^2} - 2\lambda\frac{\partial f}{\partial s} + \lambda^2 f - \frac{\partial f}{\partial s}\Big|_{s=s_1}\delta(s-s_1)\right] \quad , \quad f(s) = N\mu(s) - d_p = N[\mu(s) - \mu(s_1)]$$

gives the distributions shown in figure 6.32 in the case when $\mu$ just decays exponentially.

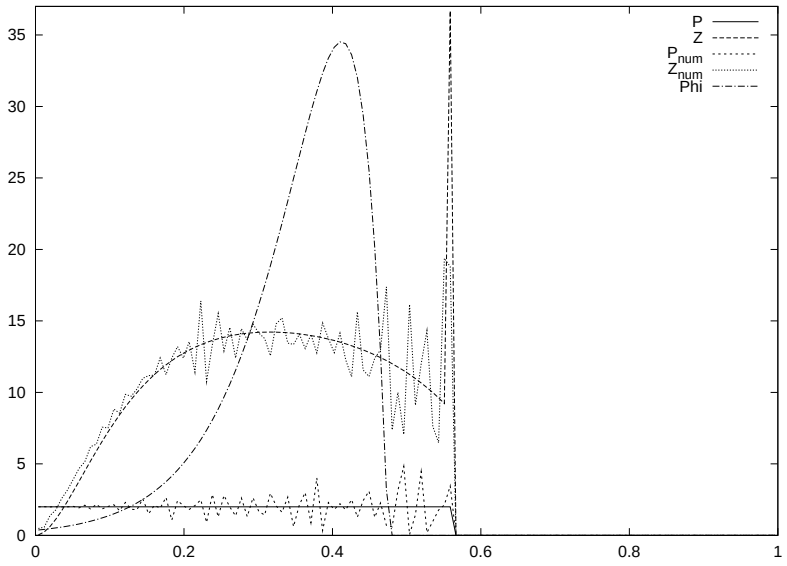

Figure 6.32: the case with $\phi(x) \sim x \exp(-\lambda x)$; here the numerical solution is shown at 5000 yrs with $dr = ds = 1/64$.

When $\mu$ is also peaked, the solutios become more complex, and analytic solutions are less apparent. For example, figure 6.33 shows what happens with

$$\mu = (1 - e^{-r})^{\alpha}\ e^{-\beta r}$$

and the $\Phi$ function 6.29.

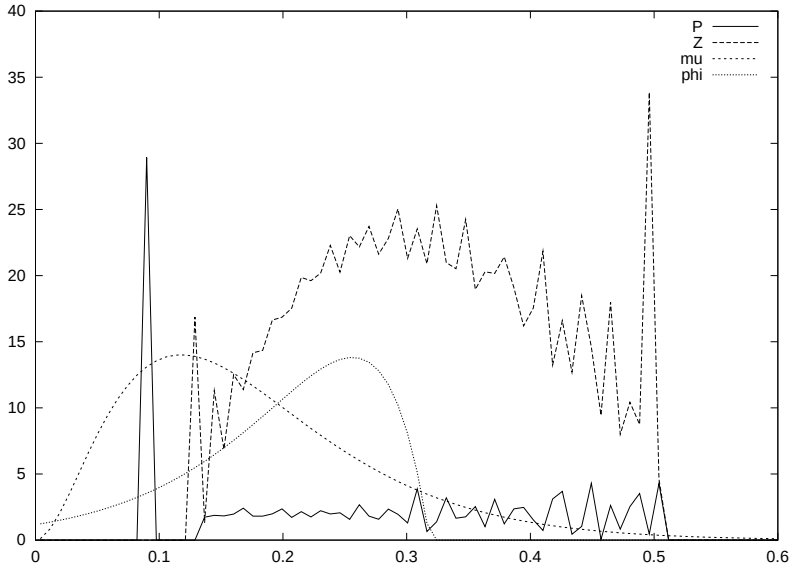


Figure 6.33: a case with both grazing and uptake having peaks. $\lambda = 16$, $\alpha = 2$, $\beta = 16$; solid: $P$, dashed: $Z$, dotted: $\mu$, dot-dash $\Phi$ (scaled).

We can examine the development of this kind of structure by starting with a wide grazing kernel and a narrow uptake function and then broadening the latter (figure 6.34).

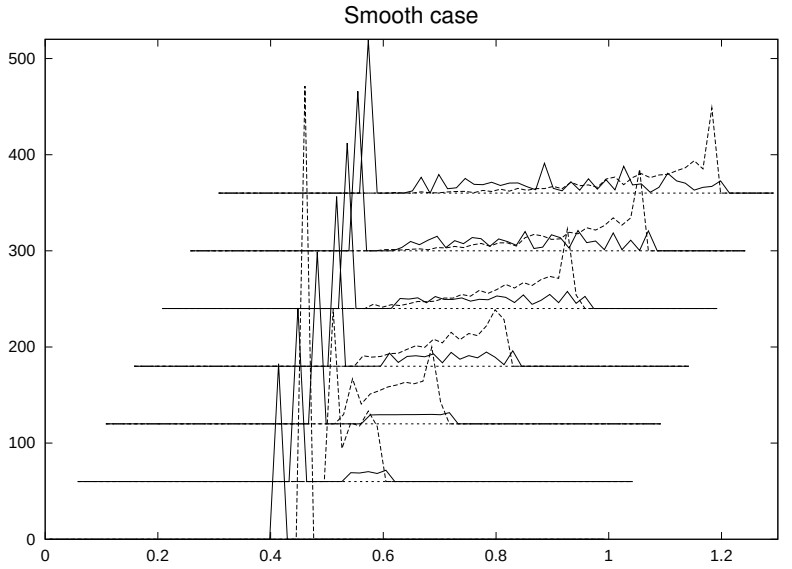

Figure 6.34: a sequence with $\alpha = 96, 32, 16, 8, 4, 2, 1$ and $\beta = 2\alpha$ with solid: $5 \times P$, dashed: $Z$. The offset of the plots to the right and upward somewhat obscures the fact that the sigular $P$ solution is shifting to lower $r$ values. The continuum solutions would settle to a constant curve like that for $\alpha = 16$ given a long enough time, although these were integrated for 10,000 yrs. The singularity in $Z$ at low $s$ seems to disappear as the continuum solution broadens, but one develops at the maximum $s$ value, as in fig. 6.33.

However, the shape of the grazing kernel can make a significant difference. We have also looked at the case with a $\Phi$ which decays exponentially in both directions (though not symmetrically) but does not cut off:

$$\Phi = [1 + \tanh(5\beta(s - r))][1 + \tanh(-\beta(s - r))];$$

The resulting patterns are much more like the discrete solutins found in section 6.2.4. The solutions in the case of an uptake function much wider than the grazing kernel appear to be approaching a discrete set of $P$ and $Z$ values, but extremely slowly.

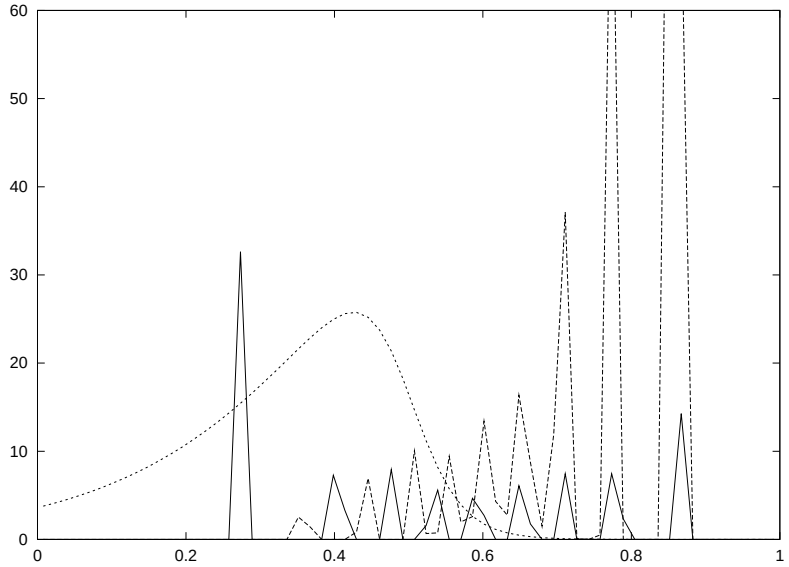


Figure 6.35: a sequence with $\alpha = 32, 24, 16, 8, 4, 2, 1$ and $\beta = 2\alpha$ with the double tanh profile.

To illustrate this point, we plot results for two very similar grazing kernels. Even though both sets are noisy, in figure 6.36. When the grazing kernel becomes narrow, many of the traits become populated. The shape of the kernel still seems to matter: for one with a cut-off (as used above), the distribution becomes continuous, albeit the time needed to reach smooth curves is very long. But for a kernel which decays exponentially in both directions, even nonsymmetrically, the distributions remain "spiky," suggesting that the final state might be a set of singular points. Here, they are smoothed out by the numerics and the finite integration time.

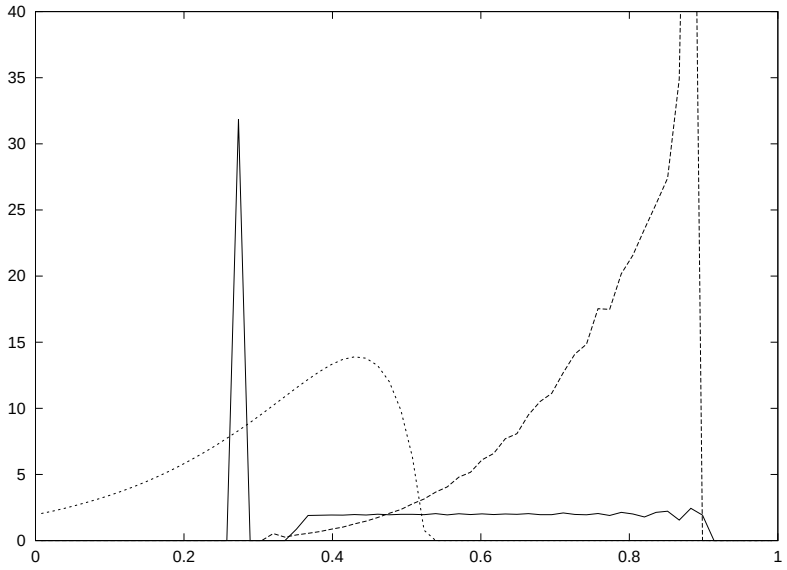


Figure 6.36a: Solutions with a kernel which cuts off when $s > \text{const} \times r$ (illustrated by one example $\phi$ curve ($t = 100,000$ yrs.

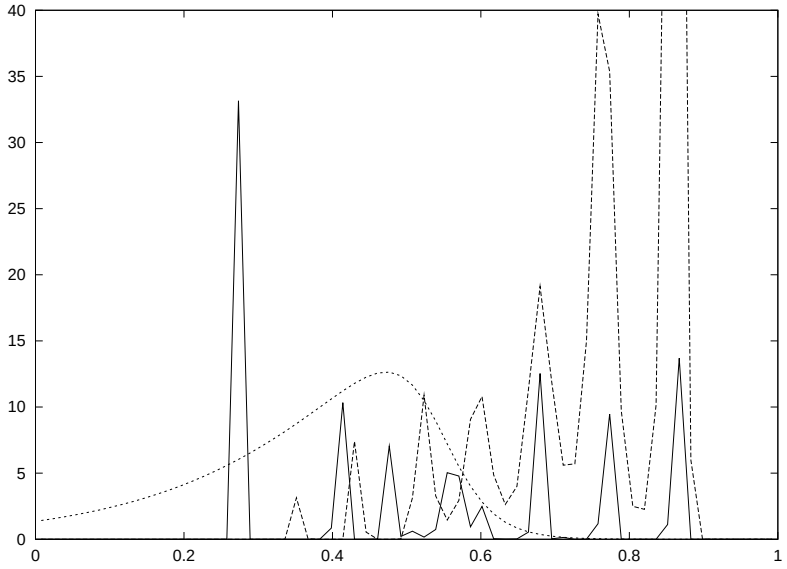


Figure 6.36b: Solutions with a kernel which decays smoothly for $s >> r$ (illustrated by one exaple $\phi$ curve.

### 6.5.6 — Omnivores

We can include omnivory and carnivory by going back to equation 6.22 but using a 2D trait space, with $r$ corresponding to log weight and $n$ ranging from 0 for autotrophs to 1 for hetereotrophs

$$\frac{1}{b(r,n)}\frac{\partial}{\partial t}b(r,n) = \mu(r,n)N - d(r,n) + \int dr'[aG(r,n|r',n') - G(r',n'|r,n)]b(r',n')$$

We begin with the simple case where $n = 0$ or 1 only (either auto- or heterotroph) and assume that anything within the prey size range is preyed upon equally, with no distinction between PP and ZP. Then we have

$$\frac{1}{P}\frac{\partial}{\partial t}P = \mu(r)N - d_p(r) - \int ds\ \Phi(s-r)g_0(s)Z(s)$$
$$\frac{1}{Z}\frac{\partial}{\partial t}Z = a(s)g_0(s)\int dr\ \Phi(s-r)[P(r)+Z(r)] - \int dr\ \Phi(r-s)g_0(r)Z(r) - d_z(s)$$

As an example, we show the structure for the $(s-r)exp(-\lambda[s-r])(s>r)$ form (figure 6.37) with the allometric terms proportional to $\exp(-10s)$; the ZP extend over a wider range, and, as figure 6.37b shows, the ones at large $s$ values are supported by consuming the smaller ZP.

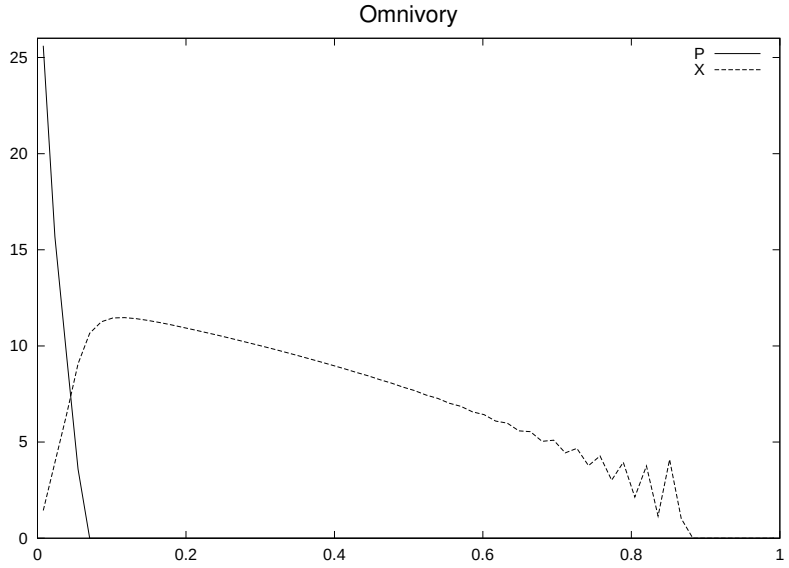


Fig. 6.37a: Case with ominvorous ZP. Feeding does not depend on whther the source is PP$orSZ$. The noise at the end is clearly discretization error; it is in steady state.

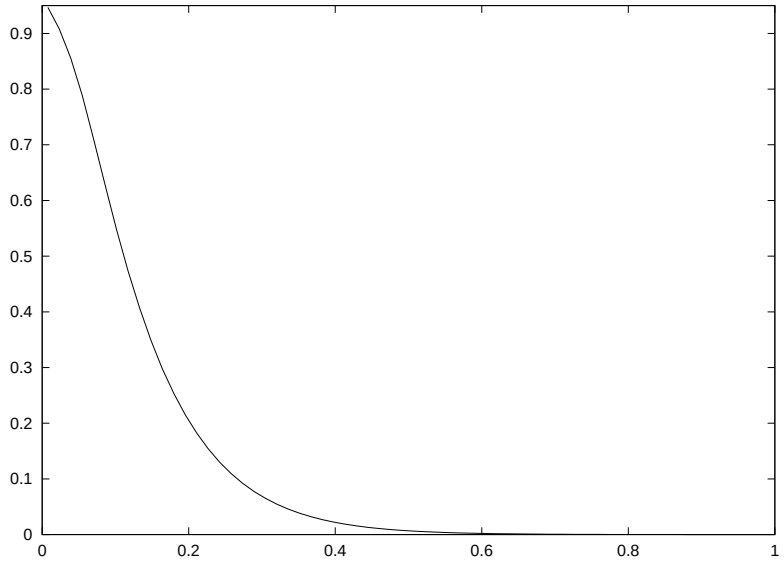


Fig. 6.37b: Fraction of food for $Z(s)$ from the PP.

The very small ZP may only be able to capture and assimilate PP, while the largest organisms are entirely carnivores. Of course, the world does not work this way, just as feeding is not a strict function of the ratio of prey to predator weight. We can add a preference, $p(s)$, for ZP in class $s$ for PP, with $1 - p(s)$ being the preference for ZP as food. Figure 6.38 shows the not-surprising result – which will be quite sensitive to the shape of the preference curve – that the zooplanton separate into two overlapping groups depending on their food source.

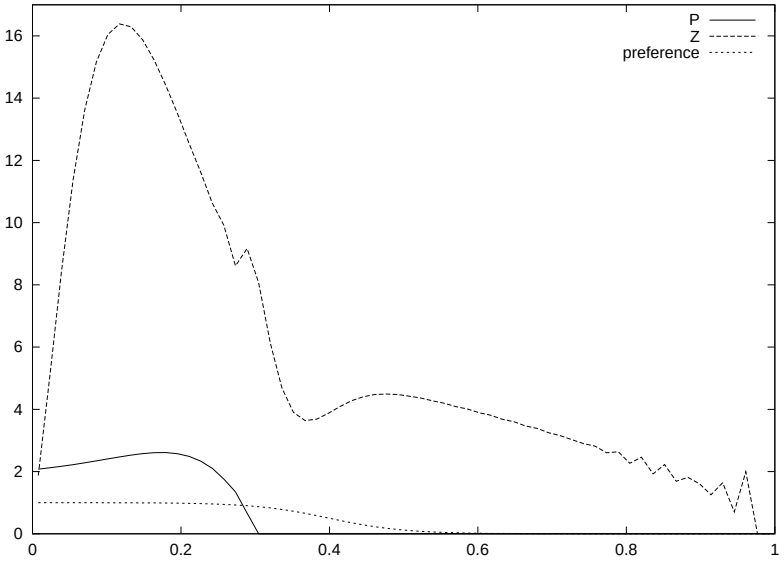


Fig. 6.38: $P$ and $Z$ vs. log weight with preference of small $Z$ for $P$ only and large $Z$ for $Z$.

As a final example, we consider a case it which the grazing kernel starts when the prey weight is some fraction of the predator weight, e.g.

$$\Phi \sim (s - r - \alpha)\, e^{-\lambda(s-r-\alpha)}\, (s > r + \alpha)$$

Numerically, the previous version was posed with a very small negative offset so that the bin with $r = s$ had a non-zero value; this could be viewed as a form of competition rather than cannabalism. But when $\alpha$ is positive and not small compared to the descretization, the ZP distribution is no longer smooth (figure 6.39). Local competition appears to be at work here: predators in one area seem to suppress smaller competitors until $\Phi$ is too small. But competitive exclusion acts very slowly when the traits are very similar, so the $P$ and $Z$ distributions change noticeably on time scales of 100 years even after intergations for $10^6$ years.

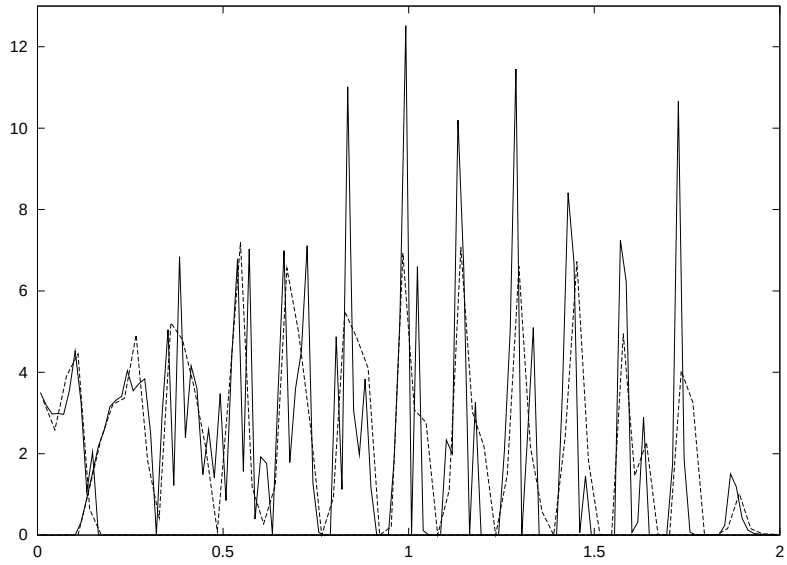


Fig. 6.39: Case with gap in size between predator and prey. Computations with 128 size classes (solid) and 64 classes (dashed) are shown.